Distributed Control of Spacecraft Formations via Cyclic Pursuit: Theory and Experiments

Jaime L. Ramirez [*], Marco Pavone [†], Emilio Frazzoli [‡], David W. Miller [§]

Massachusetts Institute of Technology

77 Massachusetts Avenue, Cambridge, MA 02139, U.S.A

In this paper we study distributed control policies for spacecraft formations that draw inspiration from the simple idea of cyclic pursuit. First, we study cyclic-pursuit control laws for both single- and double-integrator models in three dimensions. In particular, we develop control laws that only require relative measurements of position and velocity with respect to the two leading neighbors in the ring topology of cyclic pursuit, and allow convergence to a variety of symmetric formations, including evenly spaced circular and elliptic formations, and evenly spaced Archimedes' spirals. Second, we discuss potential applications, including spacecraft formation for interferometric imaging and convergence to low-effort relative trajectories. Finally, we present and discuss experimental results obtained by implementing the aforementioned control laws on the SPHERES testbed on board the International Space Station.

I. Introduction

In recent years, the idea of *distributing* the functionalities of a complex agent among multiple, simple and cooperative agents is attracting increasing interest in several application

[*]Ph.D. Candidate, Department of Aeronautics and Astronautics, Massachusetts Institute of Technology, AIAA Student Member.

[†]Ph.D. Candidate, Department of Aeronautics and Astronautics, Massachusetts Institute of Technology.

[‡]Associate Professor, Department of Aeronautics and Astronautics, Massachusetts Institute of Technology, AIAA Senior Member.

[§]Professor and Director of the Space Systems Lab, Department of Aeronautics and Astronautics, Massachusetts Institute of Technology, AIAA Senior Member.

domains. In fact, multi-agent systems present several advantages. For example, considering an aerospace application, a cluster of spacecraft flying in formation for high-resolution, synthetic-aperture imaging can act as a sparse aperture with an effective dimension larger than the one that can be achieved by a single, larger satellite.[1] In general, the intrinsic parallelism of a multi-agent system provides robustness to failures of single agents; moreover, it is possible to reduce the total implementation and operation cost, increase reactivity and system reliability, and add flexibility and modularity to monolithic approaches.

In this context, the problem of formation of *geometric patterns* is of particular interest, with engineering applications including distributed sensing using mobile sensor networks, and space missions with multiple spacecraft flying in formation (on which we will focus the paper). Within the robotics community, many distributed control strategies have been recently proposed for convergence to geometric patterns. Justh *et al.*[6] presented two strategies to achieve, respectively, rectilinear and circular formation, using all-to-all communication among agents. Jadbabaie *et al.*[7] formally proved that the nearest neighbor algorithm by Vicsek[8] causes all agents to eventually move in the same direction, despite the absence of centralized coordination and despite the fact that each agent's set of nearest neighbors change with time as the system evolves. Olfati-Saber *et al.*[9] and Leonard *et al.*[10] used potential function theory to prescribe flocking behavior in connected graphs. Lin *et al.*[11] exploited cyclic pursuit (where each agent i pursues the next $i+1$, modulo n) to achieve alignment among agents, while Marshall *et al.*[12,13] extended the classic cyclic pursuit to a system of wheeled vehicles, each subject to a single non-holonomic constraint, and studied the possible equilibrium formations and their stability. Paley *et al.*[14] introduced control strategies to stabilize symmetric formations on convex, closed curves. Ren[15,16] introduced Cartesian coordinate coupling to existing consensus algorithms and derived algorithms for different types of collective motions (a more detailed discussion on the two-part paper[15,16] is given in Section IV.C).

The problem of formation of geometric patterns has been the subject of intensive research efforts also within the aerospace community, see[17] and references therein; see also the very recent work of Chung et al.,[18] where the authors present a contraction theory approach to achieve synchronized formations that, however, requires a form of higher level agreement on the set of predetermined trajectories. Broadly speaking, spacecraft formation algorithms can be divided into three main architectures:[17] (i) Multiple-Input Multiple-Output (MIMO), in which the formation is treated as a single multiple-input, multiple-output plant, (ii) Leader/Follower, in which individual spacecraft controllers are connected hierarchically, and (iii) Cyclic, in which individual spacecraft controllers are connected non-hierarchically. By allowing non-hierarchical connections between individual spacecraft controllers, Cyclic algorithms can perform better than Leader/Follower algorithms, and can distribute control effort more evenly.[17] Moreover, Cyclic algorithms are generally more robust than MIMO algorithms, for which a local failure can have a global effect.[17] Finally, Cyclic algorithms can also be completely decentralized in the sense that there is neither a coordinating agent nor instability resulting from single point failures.[17] The two primary drawbacks of Cyclic algorithms are that the stability of these algorithms and their information requirements are poorly understood;[17] in particular, the stability analysis of Cyclic algorithms is difficult since the cyclic structure introduces feedback paths.

Motivated by the previous discussion, the objective of this paper is to present a class of Cyclic algorithms for formation flight, for which a rigorous stability analysis is possible and for which the information requirements are minimal. The starting point is our previous work,[4] where we developed distributed control policies that draw inspiration from the simple idea of cyclic pursuit and that guarantee convergence to symmetric formations. The key features of the control laws in[4] are global stability and the capability to achieve a variety of formations, namely rendez-vous to a single point, circles, and logarithmic spirals; moreover, the control laws in[4] are distributed and require the minimum number of communication links (n links for n agents) that a cyclic structure can have.

Specifically, the main contributions of this paper are threefold. First, building upon the work in,[4] we rigorously study novel cyclic-pursuit control laws for formation flight, for both single- and double-integrator models in three dimensions. We also extend our control laws to deal with the (linearized) relative dynamics of spacecraft, e.g., in the Earth's gravitational field. In particular, unlike the work of Chung et al.,[18] our control laws do not require any agreement on a set of predetermined trajectories. Second, we discuss potential applications, including spacecraft formation for interferometric imaging and convergence to low-effort relative trajectories. Finally, we present and discuss experimental results obtained by implementing the aforementioned control laws on the SPHERES testbed[21] on board the International Space Station.

The organization of this paper is as follows. In Section II, we introduce basic concepts in matrix theory and review the cyclic-pursuit control laws in,[4] which were devised for single-integrator models in two dimensions. In Section III, we extend the aforementioned control laws in three directions: (i) we address the case in which agents move in three dimensions, (ii) we consider control of the center of the formation, and (iii) we study convergence to evenly-spaced circular formations with a prescribed radius. Then, in Section IV, we extend the control laws in[4] to double-integrator models in three dimensions. In particular, we develop control laws that only require *relative* measurements of position and velocity with respect to the two leading neighbors in the ring topology of cyclic pursuit, and allow the agents to converge from *any* initial condition (except for a set of measure zero) to a single point, an evenly-spaced circular formation, an evenly-spaced logarithmic spiral formation, or an evenly-spaced Archimedes' spiral formation (an Archimedes' spiral is a spiral with the property that successive turnings have a constant separation distance), depending on some tunable control parameters. Control laws that only rely on relative measurements are indeed of critical importance in deep-space missions, where global measurements may not be available. In Section V, we discuss potential applications, including spacecraft formation for interferometric imaging and convergence to zero-effort orbits, and we argue that Archimedes' spiral formations are among the most useful symmetric formations for applications. Finally, in Section VI, we present and discuss experimental results obtained by implementing the proposed control laws on three nanospacecraft on board the International Space Station (ISS), and in Section VII we draw our conclusions.

II. Background

In this section, we provide some definitions and results from matrix theory. Moreover, we briefly review cyclic-pursuit control laws for single integrators.

A. Notation

We let $\mathbb{R}_{>0}$ and $\mathbb{R}_{\geq 0}$ denote the positive and nonnegative real numbers, respectively. We let I_n denote the identity matrix of size n; we let A^T and A^* denote, respectively, the transpose and the conjugate transpose of a matrix A. For an $n \times n$ matrix A, we let $\mathrm{eig}(A)$ denote the set of eigenvalues of A, and we refer to its kth eigenvalue as $\lambda_{A,k}$, $k \in \{1, \dots, n\}$ (or simply as λ_k when there is no possibility of confusion). Finally, let $j \doteq \sqrt{-1}$.

B. Kronecker Product

Let A and B be $m \times n$ and $p \times q$ matrices, respectively. Then, the Kronecker product $A \otimes B$ of A and B is the $mp \times nq$ matrix

$$A \otimes B = \begin{bmatrix} a_{11}B & \dots & a_{1n}B \\ \vdots & & \vdots \\ a_{m1}B & \dots & a_{mn}B \end{bmatrix}.$$

If λ_A is an eigenvalue of A with associated eigenvector ν_A and λ_B is an eigenvector of B with associated eigenvector ν_B, then $\lambda_A \lambda_B$ is an eigenvalue of $A \otimes B$ with associated eigenvector $\nu_A \otimes \nu_B$. Moreover, the following property holds: $(A \otimes B)(C \otimes D) = AC \otimes BD$, where A, B, C and D are matrices with appropriate dimensions.

C. Determinant of Block Matrices

If A, B, C and D are matrices of size $n \times n$, and $AC = CA$, then

$$\det\left(\begin{bmatrix} A & B \\ C & D \end{bmatrix}\right) = \det(AD - CB). \tag{1}$$

D. Rotation Matrices

A rotation matrix is a real square matrix whose transpose is equal to its inverse and whose determinant is $+1$. The eigenvalues of a rotation matrix in two dimensions are $e^{\pm j\alpha}$, where α is the magnitude of the rotation. The eigenvalues of a rotation matrix in three dimensions are 1 and $e^{\pm j\alpha}$, where α is the magnitude of the rotation about the rotation axis; for a rotation about the axis $(0, 0, 1)^T$, the corresponding eigenvectors are $(0, 0, 1)^T, (1, +j, 0)^T (1, -j, 0)^T$.

E. Circulant Matrices

A circulant matrix C is an $n \times n$ matrix having the form

$$C = \begin{bmatrix} c_0 & c_1 & c_2 & \dots & c_{n-1} \\ c_{n-1} & c_0 & c_1 & \dots & \vdots \\ \vdots & & & & c_1 \\ c_1 & c_2 & \dots & \dots & c_0 \end{bmatrix}. \tag{2}$$

The elements of each row of C are identical to those of the previous row, but are shifted one position to the right and wrapped around. A detailed treatise on circulant matrices can be found in.[20] The following theorem summarizes some of the properties of circulant matrices and will be essential in the development of the paper.

Theorem II.1 (Adapted from Theorem 7 in[20]) *Every $n \times n$ circulant matrix C has eigenvectors*

$$\psi_k = \frac{1}{\sqrt{n}} \left(1, e^{2\pi jk/n}, \dots, e^{2\pi jk(n-1)/n}\right)^T, \quad k \in \{0, 1, \dots, n-1\}, \tag{3}$$

and corresponding eigenvalues

$$\lambda_k = \sum_{p=0}^{n-1} c_p e^{2\pi jkp/n}, \tag{4}$$

and can be expressed in the form $C = U\Lambda U^*$, where U is a unitary matrix whose kth column is the eigenvector ψ_k, and Λ is the diagonal matrix whose diagonal elements are the corre-

sponding eigenvalues. Moreover, let C and B be $n \times n$ circulant matrices with eigenvalues $\{\lambda_{B,k}\}_{k=1}^{n}$ and $\{\lambda_{C,k}\}_{k=1}^{n}$, respectively; then,

1. *C and B commute, that is, $CB = BC$, and CB is also a circulant matrix with eigenvalues* $\text{eig}(CB) = \{\lambda_{C,k}\,\lambda_{B,k}\}_{k=1}^{n}$*;*

2. *$C + B$ is a circulant matrix with eigenvalues* $\text{eig}(C + B) = \{\lambda_{C,k} + \lambda_{B,k}\}_{k=1}^{n}$.

From Theorem II.1 all circulant matrices share the same eigenvectors, and the same matrix U diagonalizes *all* circulant matrices.

F. Cyclic Pursuit for Single Integrators

Let there be n ordered mobile agents [a] in the plane, their positions at time $t \geq 0$ denoted by $\mathbf{x}_i(t) = [x_{i,1}(t), x_{i,2}(t)]^T \in \mathbb{R}^2$, $i \in \{1, 2, \dots, n\}$, where agent i pursues the next $i+1$ modulo[b] n. The dynamics of each agent is described by a simple (vector) integrator:[4]

$$
\begin{aligned}
\dot{\mathbf{x}}_i &= \mathbf{u}_i, \\
\mathbf{u}_i &= R(\alpha)(\mathbf{x}_{i+1} - \mathbf{x}_i),
\end{aligned}
\tag{5}
$$

where the dot represents differentiation with respect to time, and $R(\alpha)$, $\alpha \in [-\pi, \pi)$, is the rotation matrix:

$$
R(\alpha) = \begin{pmatrix} \cos\alpha & \sin\alpha \\ -\sin\alpha & \cos\alpha \end{pmatrix}.
$$

Let $\mathbf{x} = [\mathbf{x}_1^T, \mathbf{x}_2^T, \dots, \mathbf{x}_n^T]^T$; the dynamics of the overall system can be written in compact form as

$$
\dot{\mathbf{x}} = (L \otimes R(\alpha))\,\mathbf{x},
$$

where L is the circulant matrix

$$
L = \begin{bmatrix} -1 & 1 & 0 & \dots & 0 \\ 0 & -1 & 1 & \dots & 0 \\ \vdots & & & & \vdots \\ 1 & 0 & 0 & \dots & -1 \end{bmatrix}.
\tag{6}
$$

From Theorem II.1 the eigenvalues of matrix L are $\{e^{2\pi jk/n} - 1\}_{k=1}^{n}$. Then, by the properties of the Kronecker product, the $2n$ eigenvalues of $L \otimes R(\alpha)$ are $\{(e^{2\pi jk/n} - 1)e^{\pm j\alpha}\}_{k=1}^{n}$. The following is proven in:[4]

[a]Henceforth, we will use the words agent and spacecraft interchangeably.
[b]Henceforth, agent indices should be evaluated modulo n.

Theorem II.2 *$L \otimes R(\alpha)$ has exactly two zero eigenvalues, and*

1. *if $0 \leq |\alpha| < \pi/n$, all non-zero eigenvalues lie in the open left-half complex plane;*
2. *if $|\alpha| = \pi/n$, two non-zero eigenvalues lie on the imaginary axis, while all other non-zero eigenvalues lie in the open left-half complex plane;*
3. *if $\pi/n < |\alpha| < 2\pi/n$, two non-zero eigenvalues lie in the open right-half complex plane, while all other non-zero eigenvalues lie in the open left-half complex plane;*

Moreover, it is possible to prove (see ref.[4]) that the matrix $L \otimes R(\alpha)$ is diagonalizable for all values of α. Then, by exploiting the structure of the eigenvectors of a circulant matrix (see Theorem II.1), it is easy to show[4] that agents starting at any initial condition (except for a set of measure zero) in $\mathbb{R}^{2n}$ and evolving under (5) exponentially converge:

1. if $0 \leq |\alpha| < \pi/n$, to a single limit point, namely their initial center of mass;
2. if $|\alpha| = \pi/n$, to an evenly spaced circle formation;
3. if $\pi/n < |\alpha| < 2\pi/n$, to an evenly spaced logarithmic spiral formation.

Note that (i) these results are derived for agents operating in $\mathbb{R}^2$ and with single-integrator dynamics, (ii) the center of the formation is determined by the initial positions of the agents, and (iii) the radius of a circular formation is also determined by the initial positions of the agents.

III. Cyclic-Pursuit Control Laws for Single-Integrator Models

In this section, we extend the results in[4] in three directions: (i) we address the case in which agents move in $\mathbb{R}^3$, (ii) we consider control of the center of the formation, and (iii) we study convergence to evenly-spaced circular formations with a prescribed radius. We start by addressing issues (i) and (ii).

A. Cyclic pursuit in three dimensions with control on the center of the formation

Let there be n ordered mobile agents in the space, their positions at time $t \geq 0$ denoted by

$$\mathbf{x}_i(t) = [x_{i,1}(t), x_{i,2}(t), x_{i,3}(t)]^T \in \mathbb{R}^3, \quad i \in \{1, 2, \ldots, n\},$$

and let $\mathbf{x} = [\mathbf{x}_1^T, \mathbf{x}_2^T, \ldots, \mathbf{x}_n^T]^T$. The dynamics of each agent are described by a simple vector integrator

$$\dot{\mathbf{x}}_i = k_g \, \mathbf{u}_i, \quad k_g \in \mathbb{R}_{>0}; \tag{7}$$

henceforth, without loss of generality, we assume $k_g = 1$. Consider the following three-dimensional generalization of the cyclic-pursuit control law in equation (5):

$$\mathbf{u}_i = R(\alpha)(\mathbf{x}_{i+1} - \mathbf{x}_i) - k_c\,\mathbf{x}_i, \quad k_c \in \mathbb{R}_{\geq 0}, \tag{8}$$

where $R(\alpha)$, $\alpha \in [-\pi,\, \pi)$, is the rotation matrix (with rotation axis $(0, 0, 1)^T$ without loss of generality):

$$R(\alpha) = \begin{pmatrix} \cos\alpha & \sin\alpha & 0 \\ -\sin\alpha & \cos\alpha & 0 \\ 0 & 0 & 1 \end{pmatrix}. \tag{9}$$

The overall system can be written in compact form as

$$\dot{\mathbf{x}} = (L \otimes R(\alpha) - k_c\, I_{3n})\,\mathbf{x}, \tag{10}$$

where L is defined in equation (6).

We start the analysis with the following theorem, that characterizes the spectrum of $L \otimes R(\alpha)$.

Theorem III.1 *$L \otimes R(\alpha)$ has exactly three zero eigenvalues, and*

1. *if $0 \leq |\alpha| < \pi/n$, all non-zero eigenvalues lie in the open left-half complex plane;*
2. *if $|\alpha| = \pi/n$, two non-zero eigenvalues lie on the imaginary axis, while all other non-zero eigenvalues lie in the open left-half complex plane;*
3. *if $\pi/n < |\alpha| < 2\pi/n$, two non-zero eigenvalues lie in the open right-half complex plane, while all other non-zero eigenvalues lie in the open left-half complex plane.*

Moreover, $L \otimes R(\alpha)$ is diagonalizable for all $\alpha \in [-\pi,\, \pi)$.

Proof: By the properties of the Kronecker product, the $3n$ eigenvalues of $L \otimes R(\alpha)$ are:

$$\begin{aligned} \lambda_k &= e^{2\pi jk/n} - 1, \\ \lambda_k^+ &= (e^{2\pi jk/n} - 1)\, e^{j\alpha}, \\ \lambda_k^- &= (e^{2\pi jk/n} - 1)\, e^{-j\alpha}, \end{aligned} \tag{11}$$

where $k \in \{1, \ldots, n\}$. Note that for $k \in \{1, \ldots, n-1\}$ the eigenvalues λ_k lie in the open left-half complex plane, while for $k = n$ we have $\lambda_n = 0$; moreover, the $2n$ eigenvalues $\{\lambda_k^\pm\}_{k=1}^n$ are the same as those in Theorem II.2. Then, the first part of the claim follows from Theorem II.2.

We now turn our attention to the diagonalizability of $L \otimes R(\alpha)$. We already now that $L \otimes R(\alpha)$ has three zero eigenvalues; note that the zero eigenvalues are all obtained for $k = n$. Next, we study the algebraic multiplicity of the eigenvalues obtained for $k < n$ (if any, i.e., if $n > 1$). The magnitude of the eigenvalues λ_k, $k \in \{1, \ldots, n\}$, is given by

$$|\lambda_k| = \sqrt{\Big(\cos(2\pi k/n) - 1\Big)^2 + \sin^2\Big(2\pi k/n\Big)} = \sqrt{2\,\Big(1 - \cos(2\pi k/n)\Big)} = 2\,\sin\frac{\pi k}{n}.$$

Note that the eigenvalues λ_k^+ (respectively λ_k^-) are just a rotation with angle α (respectively $-\alpha$) of the eigenvalues λ_k (in particular $|\lambda_k^\pm| = \lambda_k$ for every k); hence, as α is varied, the eigenvalues $\lambda_k^\pm$ move on circles with radius $r_k = 2\sin(\pi k/n)$ and center the origin. Since it holds

$$\sin\Big(\pi(n-k)/n\Big) = \sin\left(\pi k/n\right), \tag{12}$$

there are only $(n-1)/2$ distinct circles if n is odd, or $n/2$ distinct circles if n is even; we call C_k such circles, $k \in \{1, \ldots, \bar{k}\}$, where $\bar{k} = (n-1)/2$ if n is even and $\bar{k} = n/2$ otherwise. From equation (12), the eigenvalues that lie on the same circle C_k are, for all $\alpha \in [-\pi, \pi)$,

$$\lambda_k, \quad \lambda_{n-k}, \quad \lambda_k^+, \quad \lambda_{n-k}^+, \quad \lambda_k^-, \quad \lambda_{n-k}^-, \quad k = 1, 2, \ldots, \bar{k}; \tag{13}$$

Therefore just 6 eigenvalues lie on the same circle (3 in the case that n is even and $k = \bar{k}$). Clearly, only the eigenvalues that lie on the same circle can coincide.

Assume that n is odd, or n is even and $k < \bar{k}$. Then, the eigenvalues λ_k and λ_{n-k} are distinct. Indeed, $\lambda_k = \lambda_{n-k}$ implies $\sin(2\pi k/n) = \sin(2\pi(n-k)/n)$; since we have

$$0 < 2\pi k/n < 2\pi \quad \text{for} \quad k \in \{1, \ldots, n-1\},$$

the equality $\sin(2\pi k/n) = \sin(2\pi(n-k)/n)$ is impossible under the assumptions. Similarly, the eigenvalues λ_k^+ and λ_{n-k}^+ are distinct, and the eigenvalues λ_k^- and λ_{n-k}^- are distinct. As α is changed, the eigenvalues λ_k and λ_{n-k}, which are distinct, do not move along the circle C_k; as α is increased, the eigenvalues λ_k^+ and λ_{n-k}^+, which are distinct, move counter-clockwise along the circle C_k, with fixed (non-zero) phase difference; finally, as α is increased, the eigenvalues λ_k^- and λ_{n-k}^-, which are distinct, move clockwise along the circle C_k, with fixed (non-zero) phase difference. We conclude that at most three eigenvalues can coincide; in particular, the possible pairs of eigenvalues that can coincide are

$$\begin{gathered}(\lambda_k, \lambda_k^+), \quad (\lambda_k, \lambda_{n-k}^+), \quad (\lambda_k, \lambda_k^-), \quad (\lambda_k, \lambda_{n-k}^-), \quad (\lambda_{n-k}, \lambda_k^+), \quad (\lambda_{n-k}, \lambda_{n-k}^+), \quad (\lambda_{n-k}, \lambda_k^-), \\ (\lambda_{n-k}, \lambda_{n-k}^-), \quad (\lambda_k^+, \lambda_k^-), \quad (\lambda_k^+, \lambda_{n-k}^-), \quad (\lambda_{n-k}^+, \lambda_k^-), \quad (\lambda_{n-k}^+, \lambda_{n-k}^-).\end{gathered} \tag{14}$$

Similarly, the only triples of eigenvalues that can potentially coincide are

$$\lambda_k \longrightarrow \begin{cases} \lambda_k^+ & \longrightarrow \begin{cases} \lambda_k^- \\ \lambda_{n-k}^- \end{cases} \\ \lambda_{n-k}^+ & \longrightarrow \begin{cases} \lambda_k^- \\ \lambda_{n-k}^- \end{cases} \end{cases} \quad \text{and} \quad \lambda_{n-k} \longrightarrow \begin{cases} \lambda_k^+ & \longrightarrow \begin{cases} \lambda_k^- \\ \lambda_{n-k}^- \end{cases} \\ \lambda_{n-k}^+ & \longrightarrow \begin{cases} \lambda_k^- \\ \lambda_{n-k}^- \end{cases} \end{cases} . \tag{15}$$

If n is even and $k = \bar{k}$, it is straightforward to see that the possible pairs of eigenvalues on $C_{n/2}$ that can coincide are

$$(\lambda_{n/2}, \lambda_{n/2}^+), \quad (\lambda_{n/2}, \lambda_{n/2}^-), \quad (\lambda_{n/2}^+, \lambda_{n/2}^-),$$

while the three eigenvalues on $C_{n/2}$ coincide only when $\alpha = 0$.

The last step before proving that $L \otimes R(\alpha)$ is diagonalizable is to compute its eigenvectors. Recall that the eigenvectors of L are $\psi_k = \Big(1, \chi_k, \chi_k^2, \ldots, \chi_k^{n-1}\Big)^T$, where $\chi_k = e^{2\pi j k/n}$, $k \in \{0, \ldots, n-1\}$ (we are omitting the constant $1/\sqrt{n}$). The eigenvectors of $L \otimes R(\alpha)$ are then given by

$$\begin{aligned}
\mu_k &\doteq \psi_k \otimes (0,0,1)^T = (0,0,1,0,0,\chi_k, \ldots, 0,0,\chi_k^{n-1})^T, \\
\mu_k^+ &\doteq \psi_k \otimes (1,j,0)^T = (1,j,0,\chi_k, j\,\chi_k, 0, \ldots, \chi_k^{n-1}, j\,\chi_k^{n-1}, 0)^T, \\
\mu_k^- &\doteq \psi_k \otimes (1,-j,0)^T = (1,-j,0,\chi_k, -j\,\chi_k, 0, \ldots, \chi_k^{n-1}, -j\,\chi_k^{n-1}, 0)^T,
\end{aligned}$$

where $k \in \{1, \ldots, n\}$. Given any triple of integers p, q, $r \in \{1, \ldots, k\}$, it is easy to see that the three eigenvectors μ_p, μ_q^+, μ_r^- are linearly independent (just observe the first three components of each eigenvector). Hence, the zero eigenvalues (which have an algebraic multiplicity equal to three) have a geometric multiplicity equal to three; recalling that the possible pairs or triples of non-zero coincident eigenvalues are given in equations (14) and (15), we conclude that whenever two or three eigenvalues coincide the corresponding eigenvectors are linearly independent. Therefore, $L \otimes R(\alpha)$ is diagonalizable for all $\alpha \in [-\pi, \pi)$. □

Corollary III.2 *When $\alpha = \pi/n$, the two eigenvalues that lie on the imaginary axis are $\lambda_{n-1}^+ = -j\,2\sin(\pi/n)$ and $\lambda_1^- = j\,2\sin(\pi/n)$, with corresponding eigenvectors μ_{n-1}^+ and μ_1^-. When $\pi/n < \alpha < 2\pi/n$, the two eigenvalues with positive real part are λ_{n-1}^+ and λ_1^-, with corresponding eigenvectors μ_{n-1}^+ and μ_1^-; moreover, the real parts of λ_{n-1}^+ and λ_1^- are both equal to $2\sin(\pi/n)\sin(\alpha - \pi/n)$.*

Proof: The proof reduces to a straightforward verification in equation (11). □

We are now in a position to study the formations that can be achieved with control law (8). We study separately the case with $k_c = 0$ and the case with $k_c > 0$.

1. Case $k_c = 0$, i.e., no control on the center of the formation.

Combining Theorem III.1 and Corollary III.2 (where, in particular, the eigenvectors corresponding to the dominant eigenvalues are explicitly given), it is easy to show (the arguments are virtually identical to those in Section 3.5 of[4] and are omitted in the interest of brevity) that agents starting at any initial condition (except for a set of measure zero) in $\mathbb{R}^{3n}$ and evolving under (10) exponentially converge:

1. if $0 \leq |\alpha| < \pi/n$, to a single limit point, namely their initial center of mass;

2. if $|\alpha| = \pi/n$, to an evenly spaced circle formation, whose radius is determined by the initial positions of the agents;

3. if $\pi/n < |\alpha| < 2\pi/n$, to an evenly spaced logarithmic spiral formation.

The center of the formation is determined by the initial positions of the agents. The same result has recently appeared in.[15]

Remark III.3 *When $k_c = 0$, the control law in equation (8) only requires the measurement of the relative position $(\mathbf{x}_{i+1} - \mathbf{x}_i)$; however, it uses a rotation matrix that is common to all agents. Hence, control law (8) requires that all agents agree upon a common orientation, but it does* not *require a consensus on a common origin.*

2. Case $k_c > 0$, i.e., control on the center of the formation.

We now study the case $k_c > 0$; we will see that in this case the center of the formation is no longer determined by the initial positions of the spacecraft, instead it always converges, exponentially fast, to the origin. In fact, when $k_c > 0$ the eigenvalues of $L \otimes R(\alpha)$ are shifted toward the left-hand complex plane by an amount precisely equal to k_c, while the eigenvectors are left unchanged. Then, the following corollary is a simple consequence of Corollary III.2.

Corollary III.4 *Assume $k_c > 0$; then, if $0 \leq |\alpha| \leq \pi/n$, all of the eigenvalues are in the left-hand complex plane. If, instead, $\pi/n < |\alpha| < 2\pi/n$ we have*

1. *if $k_c > 2\sin(\pi/n)\sin(\alpha - \pi/n)$, all of the eigenvalues are in the open left-hand complex plane;*

2. *if $k_c = 2\sin(\pi/n)\sin(\alpha - \pi/n)$, two non-zero eigenvalues lie on the imaginary axis, while all other eigenvalues lie in the open left-hand complex plane;*

3. *if $k_c < 2\sin(\pi/n)\sin(\alpha - \pi/n)$, two non-zero eigenvalues lie in the open right-hand complex plane, while all other eigenvalues lie in the open left-hand complex plane;*

Accordingly, by appropriately selecting α and k_c, the agents, starting at any initial condition (except for a set of measure zero) in $\mathbb{R}^{3n}$ and evolving under (10), exponentially converge to the origin, or to an evenly spaced circle formation centered at the origin, or to an evenly spaced logarithmic spiral formation centered at the origin. Simulation results are presented in Figure 1, where 7 agents reach a circular formation centered at the origin.

Remark III.5 *When $k_c > 0$, the control law in equation (8) requires that the agents agree on a common reference frame (i.e., both a common origin and a common orientation); in particular, each agent needs to measure its relative position $(\mathbf{x}_{i+1} - \mathbf{x}_i)$ and know its absolute position $\mathbf{x}_i$.*

Remark III.6 *Note that the center of the formation can be chosen to be any point in $\mathbb{R}^3$. Assume, in fact, that we desire a formation centered at $c \in \mathbb{R}^3$. Then, if we modify the control law (8) according to*

$$\mathbf{u}_i = R(\alpha)(\mathbf{x}_{i+1} - \mathbf{x}_i) - k_c\,(\mathbf{x}_i - \mathbf{x}_c), \quad k_c \in \mathbb{R}_{>0},$$

it is immediate to see that the center of the formation will converge exponentially to $\mathbf{x}_c$.

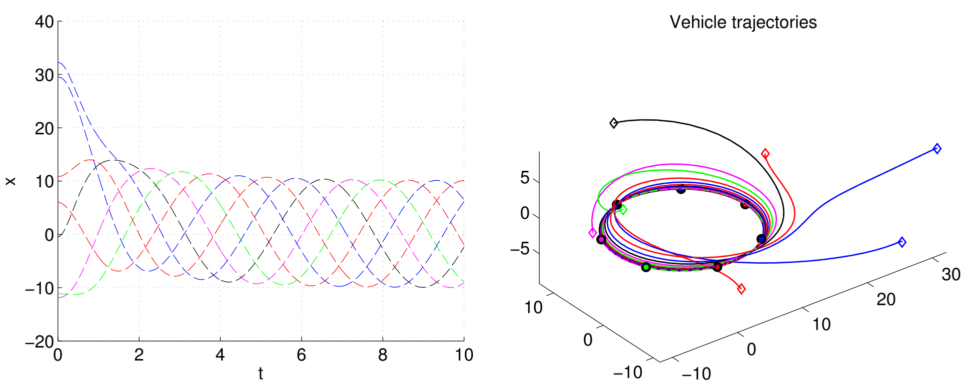

Figure 1. Convergence to circular trajectories centered at the origin. Left Figure: First coordinate as a function of time for each agent. Right Figure: Trajectories in 3D.

B. Convergence to circular formations with a prescribed radius

Circular trajectories occur only when two non-zero eigenvalues are on the imaginary axis and all other non-zero eigenvalues have negative real part, which makes this behavior not robust from a practical point of view. In this section we address the problem of *robust* convergence to a circular motion on a circle of *prescribed* radius around the (fixed) center of mass of the group, with all agents being evenly spaced on the circle. Here, by robust we mean that the circular formation is now a locally stable equilibrium of a non-linear system. The key idea is to make the rotation angle a function of the state of the system.

Specifically, let there be n ordered mobile agents in the plane, their positions at time $t \geq 0$ denoted by $\mathbf{x}_i(t) = [x_{i,1}(t), x_{i,2}(t)]^T \in \mathbb{R}^2$, $i \in \{1, 2, \ldots, n\}$, where agent i pursues the next $i+1$ modulo n. The kinematics of each agent is described by

$$\begin{aligned} \dot{\mathbf{x}}_i &= k_g\, \mathbf{u}_i, \\ \mathbf{u}_i &= R(\alpha_i)(\mathbf{x}_{i+1} - \mathbf{x}_i), \end{aligned} \tag{16}$$

where the rotation angle α_i is now a function of the state of the system:

$$\alpha_i \;=\; \frac{\pi}{n} + k_\alpha\,(r - \|\mathbf{x}_{i+1} - \mathbf{x}_i\|), \quad k_\alpha,\, r \in \mathbb{R}_{>0}. \tag{17}$$

Without loss of generality, we assume $k_g = 1$. In equation (17) the constant k_α is a gain, while r is the desired inter-agent distance. Intuitively, if the agents are "close to each other" with respect to r, they will spiral out since $\alpha_i > \pi/n$; conversely, if they are "far from each other" with respect to r, they will spiral in since $\alpha_i < \pi/n$. It is easy to see that a *splay state formation* whereby all agents move on a circle of radius $r/(2\sin(\pi/n))$ around the (fixed) center of mass of the group, with all agents being evenly spaced on the circle, is a *relative* equilibrium for the system. The next theorem shows that such equilibrium is locally stable.

Theorem III.7 *A splay-state formation is a locally stable relative equilibrium for system* (16) - (17).

Proof: We first consider a sequence of coordinate transformations such that a splay-state formation is indeed an equilibrium point (and not a *relative* equilibrium). Consider the change of coordinates $\mathbf{p}_i \doteq \mathbf{x}_{i+1} - \mathbf{x}_i$, $i \in \{1, 2, \ldots, n\}$. In the new coordinates, the system becomes (the index i is, as usual, modulo n)

$$\dot{\mathbf{p}}_i = R(\alpha_{i+1})\, \mathbf{p}_{i+1} - R(\alpha_i)\, \mathbf{p}_i, \qquad \text{where} \quad \alpha_i = \frac{\pi}{n} + k_\alpha\,(r - \|\mathbf{p}_i\|). \tag{18}$$

By introducing polar coordinates, i.e., by letting the first coordinate $p_{i,1} = \varrho_i \cos\vartheta_i$ and the second coordinate $p_{i,2} = \varrho_i \sin\vartheta_i$, with $\varrho_i \in \mathbb{R}_{\geq 0}$ and $\alpha_i \in \mathbb{R}$, the system becomes, after some algebraic manipulations (see Appendix A for the details),

$$\dot{\varrho}_i \;=\; \varrho_{i+1}\, \cos((\vartheta_{i+1} - \vartheta_i) - \alpha_{i+1}(\varrho_{i+1})) - \varrho_i\, \cos(\alpha_i(\varrho_i)), \tag{19}$$

$$\dot{\vartheta}_i \;=\; \frac{\varrho_{i+1}}{\varrho_i}\, \sin((\vartheta_{i+1} - \vartheta_i) - \alpha_{i+1}(\varrho_{i+1})) + \sin(\alpha_i(\varrho_i)), \tag{20}$$

$$\alpha_i(\varrho_i) \;=\; \frac{\pi}{n} + k_\alpha\,(r - \varrho_i), \tag{21}$$

where we have made explicit the dependence of α_i on ϱ_i. Finally, by letting $\varphi_i = \vartheta_{i+1} - \vartheta_i$, we obtain

$$\begin{aligned}
\dot{\varrho}_i &= \varrho_{i+1}\cos(\varphi_i - \alpha_{i+1}(\varrho_{i+1})) - \varrho_i\cos(\alpha_i(\varrho_i)), \\
\dot{\varphi}_i &= \frac{\varrho_{i+2}}{\varrho_{i+1}}\sin(\varphi_{i+1} - \alpha_{i+2}(\varrho_{i+2})) + \sin(\alpha_{i+1}(\varrho_{i+1})) - \frac{\varrho_{i+1}}{\varrho_i}\sin(\varphi_i - \alpha_{i+1}(\varrho_{i+1})) - \sin(\alpha_i(\varrho_i)), \\
\alpha_i(\varrho_i) &= \frac{\pi}{n} + k_\alpha(r - \varrho_i).
\end{aligned}$$

Define $\varrho \doteq (\varrho_1, \ldots, \varrho_n)^T$ and $\varphi \doteq (\varphi_1, \ldots, \varphi_n)^T$; in the new system of coordinates ϱ-φ, a splay state formation corresponds to an equilibrium *point* $\varrho^* = (r, \ldots, r)^T$ and $\varphi^* = (\frac{2\pi}{n}, \ldots, \frac{2\pi}{n}, -\frac{2\pi(n-1)}{n})^T$. In compact form we write

$$\begin{pmatrix} \dot{\varrho} \\ \dot{\varphi} \end{pmatrix} = f(\varrho, \varphi). \tag{22}$$

The linearization of system (22) around the equilibrium point (ϱ^*, φ^*) is

$$\begin{aligned}
\dot{\varrho}_i &= \cos(\pi/n)(\varrho_{i+1} - \varrho_i) - k_\alpha r\,\sin(\pi/n)(\varrho_{i+1} + \varrho_i) - r\sin(\pi/n)\,\varphi_i, \\
\dot{\varphi}_i &= (k_\alpha\cos(\pi/n) + \frac{1}{r}\sin(\pi/n))(\varrho_{i+2} - 2\varrho_{i+1} + \varrho_i) + \cos(\pi/n)(\varphi_{i+1} - \varphi_i).
\end{aligned}$$

Without loss of generality we set $r = 1$; the linearized system can be written in compact form as

$$\begin{bmatrix} \dot{\varrho} \\ \dot{\varphi} \end{bmatrix} = \begin{bmatrix} a_n\,L - 2k_\alpha\,s_n\,I_n & -s_n\,I_n \\ b_n\,L^2 & c_n\,L \end{bmatrix} \begin{bmatrix} \varrho \\ \varphi \end{bmatrix} \doteq P \begin{bmatrix} \varrho \\ \varphi \end{bmatrix},$$

where $s_n \doteq \sin(\pi/n)$, $c_n \doteq \cos(\pi/n)$, $a_n \doteq (c_n - k_\alpha s_n)$, $b_n \doteq k_\alpha c_n + s_n$, and L is defined in equation (6). The spectrum of P is characterized by the following Lemma.

Lemma III.8 *The matrix P has $2n-3$ eigenvalues with negative real part, and 3 eigenvalues with zero real part. The eigenvalues with zero real part are $\lambda_1 = 0$, and $\lambda_{2,3} = \pm 2js_n$; the corresponding eigenvectors v_1, v_2 and v_3 are:*

$$\begin{aligned}
v_1 &= (\mathbf{1}_n, -2k_\alpha\,\mathbf{1}_n)^T, \\
v_2 &= \left(\psi_1,\ -2b_n e^{\pi j/n}\psi_1\right)^T, \\
v_3 &= \bar{v}_2,
\end{aligned}$$

where $\mathbf{1}_n = (1, 1, \ldots, 1)^T \in \mathbb{R}^n$, ψ_1 is the eigenvector for $k = 1$ in equation (3) and $\bar{v}$ indicates the complex conjugate of v.

Proof: The proof of this lemma is presented in Appendix B. □

System (22) is constrained to evolve on a subset of $\mathbb{R}^{2n}$. To see why this is the case, recall that from the definition of $\mathbf{p}_i$ we have $\sum_{i=1}^{n} \mathbf{p}_i = 0$, or equivalently $\sum_{i=1}^{n} R(\vartheta_1)\mathbf{p}_i = 0$. In polar coordinates these constraints become $\sum_{i=1}^{n} \varrho_i \cos(\vartheta_i - \vartheta_1) = 0$ and $\sum_{i=1}^{n} \varrho_i \sin(\vartheta_i - \vartheta_1) = 0$. Thus, in the system of coordinates ϱ-φ, the following two constraints must hold at all time

$$g_1(\varrho, \varphi) = \sum_{i=1}^{n} \varrho_i \cos\left(\sum_{k=1}^{i-1} \varphi_k\right) = 0,$$
$$g_2(\varrho, \varphi) = \sum_{i=1}^{n} \varrho_i \sin\left(\sum_{k=1}^{i-1} \varphi_k\right) = 0.$$

Moreover, by definition of φ, the following constraint must hold at all time

$$g_3(\varrho, \varphi) = \sum_{i=1}^{n} \varphi_i = 0.$$

Let $g(\varrho, \varphi) = (g_1(\varrho, \varphi), g_2(\varrho, \varphi), g_3(\varrho, \varphi))^T$ and define

$$\mathcal{M} \doteq \{(\varrho, \varphi) \in \mathbb{R}^{2n} : g(\varrho, \varphi) = 0\} \subset \mathbb{R}^{2n}.$$

Note that $(\varrho^*, \varphi^*) \in \mathcal{M}$. The Jacobian of $g(\varrho, \varphi)$ evaluated at the equilibrium point is

$$G = \begin{pmatrix} 1 & \cos(2\pi/n) & \dots & \cos(2\pi(n-1)/n) & -\sum_{i=2}^{n} r\sin(2\pi(i-1)/n) & \dots & -r\sin(2\pi(n-1)/n) & 0 \\ 0 & \sin(2\pi/n) & \dots & \sin(2\pi(n-1)/n) & \sum_{i=2}^{n} r\cos(2\pi(i-1)/n) & \dots & r\cos(2\pi(n-1)/n) & 0 \\ 0 & 0 & \dots & 0 & 1 & \dots & 1 & 1 \end{pmatrix}.$$

Let $B_\delta(\varrho^*, \varphi^*)$ be the open ball of radius $\delta > 0$ centered at point (ϱ^*, φ^*) in $\mathbb{R}^{2n}$. The rank of G is clearly 3; then, there exists $\delta > 0$ such that $\tilde{\mathcal{M}} \doteq \mathcal{M} \cap B_\delta(\varrho^*, \varphi^*) \subset \mathbb{R}^{2n}$ is a submanifold of $\mathbb{R}^{2n}$. The tangent space of $\tilde{\mathcal{M}}$ at (ϱ^*, φ^*), that we call $T_{(\varrho^*, \varphi^*)}\tilde{\mathcal{M}}$, is an invariant subspace of P (since $\tilde{\mathcal{M}}$, by construction, is invariant under (22), i.e., $f(\varrho, \varphi) \in T_{(\varrho, \varphi)}\tilde{\mathcal{M}}$ for all $(\varrho, \varphi) \in \tilde{\mathcal{M}}$) and has dimension $2n - 3$. Pick a basis $\{w_1, \dots, w_{2n-3}\}$ of $T_{(\varrho^*, \varphi^*)}\tilde{\mathcal{M}}$ and complete it to a basis W of $\mathbb{R}^{2n}$. Then, with respect to this basis, P takes the upper-triangular form

$$\begin{bmatrix} P_{1,1} & P_{1,2} \\ 0_{3\times(2n-3)} & P_{2,2} \end{bmatrix},$$

where $0_{3\times(2n-3)}$ is the zero matrix with 3 rows and $2n - 3$ columns. Since our system is constrained to evolve, at (ϱ^*, φ^*), along the tangent space $T_{(\varrho^*, \varphi^*)}\tilde{\mathcal{M}}$, the local stability of the equilibrium point is *solely* determined by the eigenvalues of $P_{1,1}$.

We next show that the three eigenvalues of $P_{2,2}$ are exactly the three eigenvalues of P that have real part equal to zero. It is possible to show (see Appendix C) that

$$G \cdot v_i \neq 0, \quad \text{for each} \quad i \in \{1, 2, 3\},$$

where v_i, $i \in \{1,2,3\}$, are the three eigenvectors associated to the three eigenvalues with zero real part. Therefore, we have $v_i \notin T_{(\varrho^*,\varphi^*)}\tilde{\mathcal{M}}$, $i \in \{1,2,3\}$. Let y_i be the components of v_i with respect to the basis W; define $y_{i,1}$ as the vector of components with respect to $\{w_1, \ldots, w_{2n-3}\}$, and $y_{i,2}$ as the vector of components with respect to the remaining basis vectors in W. Since $v_i \notin T_{(\varrho^*,\varphi^*)}\tilde{\mathcal{M}}$, vector $y_{i,2}$ is non-zero. Since v_i is an eigenvector of P with eigenvalue λ_i, we can write

$$\begin{bmatrix} P_{1,1} & P_{1,2} \\ 0_{3\times(2n-3)} & P_{2,2} \end{bmatrix} \begin{bmatrix} y_{i,1} \\ y_{i,2} \end{bmatrix} = \lambda_i \begin{bmatrix} y_{i,1} \\ y_{i,2} \end{bmatrix},$$

and therefore $P_{2,2}\, y_{i,2} = \lambda_i\, y_{i,2}$, i.e., λ_i is an eigenvalue of $P_{2,2}$, $i \in \{1,2,3\}$. Since, we have $\operatorname{eig}(P_{1,1}) = \operatorname{eig}(P) \setminus \operatorname{eig}(P_{2,2})$, we conclude, by using Lemma III.8, that all eigenvalues of $P_{1,1}$ have negative real part. Therefore, the equilibrium point (ϱ^*, φ^*) is locally stable. □

IV. Cyclic-Pursuit Control Laws for Double-Integrator Models

In this section, we extend the previous cyclic-pursuit control laws to double integrators. We first present a control law that requires each agent to be able to measure its absolute position and velocity; then, we design a control law that only requires *relative* measurements of position and velocity. As before, let $\mathbf{x}_i(t) = [x_{i,1}(t), x_{i,2}(t), x_{i,3}(t)]^T \in \mathbb{R}^3$ be the position at time $t \geq 0$ of the ith agent, $i \in \{1, 2, \ldots, n\}$, and let $\mathbf{x} = [\mathbf{x}_1^T, \mathbf{x}_2^T, \ldots, \mathbf{x}_n^T]^T$. Moreover, let $R(\alpha)$ be the rotation matrix in three dimensions with rotation angle $\alpha \in [-\pi, \pi)$ and rotation axis $(0,0,1)^T$ (see equation (9)). The dynamics of each agent are now described by a double-integrator model:

$$\ddot{\mathbf{x}}_i = \mathbf{u}_i. \tag{23}$$

A. Dynamic Cyclic Pursuit with Reference Coordinate Frame

Consider the following feedback control law

$$\begin{aligned} \mathbf{u}_i = k_d\, R(\alpha)(\mathbf{x}_{i+1} - \mathbf{x}_i) + R(\alpha)(\dot{\mathbf{x}}_{i+1} - \dot{\mathbf{x}}_i) \\ - k_c k_d\, \mathbf{x}_i - (k_c + k_d)\, \dot{\mathbf{x}}_i, \quad k_d \in \mathbb{R}_{>0},\ k_c \in \mathbb{R}. \end{aligned} \tag{24}$$

Note that each agent needs to measure both its absolute position (if $k_c \neq 0$) and its absolute velocity (if $k_c \neq -k_d$). The overall dynamics of the n agents are described by:

$$\begin{bmatrix} \dot{\mathbf{x}} \\ \ddot{\mathbf{x}} \end{bmatrix} = \begin{bmatrix} 0 & I_{3n} \\ k_d\, A(\alpha) & A(\alpha) - k_d I_{3n} \end{bmatrix} \mathbf{x} \doteq C(\alpha)\, \mathbf{x}, \tag{25}$$

where $A(\alpha) \doteq L \otimes R(\alpha) - k_c I_{3n}$ and L is the matrix defined in equation (6). The following theorem characterizes eigenvalues and eigenvectors of $C(\alpha)$.

Theorem IV.1 *Assume that -k_d is not an eigenvalue of $A(\alpha)$. The eigenvalues of the state matrix $C(\alpha)$ in equation (25) are the union of:*

- *the $3n$ eigenvalues of $A(\alpha)$,*
- *-k_d, with multiplicity $3n$.*

In other words, eig$(C(\alpha))$ = eig$(A(\alpha)) \cup \{-k_d\}$. Moreover, the eigenvector of $C(\alpha)$ corresponding to the kth eigenvalue $\lambda_k \in$ eig$(A(\alpha))$, $k \in \{1, \ldots, 3n\}$, is:

$$\nu_k \doteq \begin{bmatrix} \nu_{k,1} \\ \nu_{k,2} \end{bmatrix} = \begin{bmatrix} \mu_k \\ \lambda_k \mu_k \end{bmatrix}, \quad k \in \{1, \ldots, 3n\},$$

where μ_k is the eigenvector of $A(\alpha)$ corresponding to λ_k. The $3n$ (independent) eigenvectors corresponding to the eigenvalue $-k_d$ (that has multiplicity $3n$) are

$$\nu_k \doteq \begin{bmatrix} \nu_{k,1} \\ \nu_{k,2} \end{bmatrix} = \begin{bmatrix} -k_d^{-1} e_{k-3n} \\ e_{k-3n} \end{bmatrix}, k \in \{3n+1, \ldots, 6n\},$$

where e_j is the jth vector of the canonical basis in $\mathbb{R}^{3n}$.

Proof: First, we compute the eigenvalues of $C(\alpha)$. The eigenvalues of $C(\alpha)$ are, by definition, solutions to the characteristic equation:

$$0 = \det \begin{bmatrix} \lambda I_{3n} & -I_{3n} \\ -k_d\, A(\alpha) & \lambda I_{3n} - (A(\alpha) - k_d I_{3n}) \end{bmatrix}.$$

By using the result in equation (1), we obtain

$$\begin{aligned} 0 &= \det\left(\lambda^2 I_{3n} - \lambda\left(A(\alpha) - k_d I_{3n}\right) - k_d\, A(\alpha)\right) \\ &= \det((\lambda + k_d) I_{3n}) \det(\lambda I_{3n} - A(\alpha)). \end{aligned}$$

Thus, the eigenvalues of $C(\alpha)$ must satisfy $0 = \det((\lambda + k_d)I_{3n})$ and $0 = \det(\lambda I_{3n} - A(\alpha))$; hence, the first part of the claim is proved.

By definition, the eigenvector $[\nu_{k,1}^T\,\nu_{k,2}^T]^T$ corresponding to the eigenvalue λ_k, $k = 1, \dots, 6n$, satisfies the eigenvalue equation:

$$\lambda_k \begin{bmatrix} \nu_{k,1} \\ \nu_{k,2} \end{bmatrix} = \begin{bmatrix} 0 & I_{3n} \\ k_d\, A(\alpha) & A(\alpha) - k_d I_{3n} \end{bmatrix} \begin{bmatrix} \nu_{k,1} \\ \nu_{k,2} \end{bmatrix}$$
$$= \begin{bmatrix} \nu_{k,2} \\ k_d\, A(\alpha)\nu_{k,1} + A(\alpha)\nu_{k,2} - k_d\nu_{k,2} \end{bmatrix}.$$

Thus, we obtain

$$\lambda_k\nu_{k,1} = \nu_{k,2},$$
$$\lambda_k\nu_{k,2} = k_d\, A(\alpha)\nu_{k,1} + A(\alpha)\nu_{k,2} - k_d\,\nu_{k,2},$$

and therefore

$$\lambda_k(k_d + \lambda_k)\nu_{k,1} = (k_d + \lambda_k)\, A(\alpha)\, \nu_{k,1}. \tag{26}$$

If $\lambda_k = -k_d$, then we have $3n$ eigenvectors given by $[-k_d^{-1}e_j,\ e_j]^T$, $j = \{1, \dots, 3n\}$. If, instead, $\lambda_k \in \text{eig}(A(\alpha))$ (note that by assumption $-k_d \notin \text{eig}(A(\alpha))$), we obtain from equation (26)

$$\lambda_k\nu_{k,1} = A(\alpha)\nu_{k,1},$$

and we obtain the claim. □

We are now in a position to study the formations that can be achieved with control law (24).

Theorem IV.2 *Assume that -k_d is not an eigenvalue of $A(\alpha)$. Then, agents' positions starting at any initial condition (except for a set of measure zero) in $\mathbb{R}^{3n}$ and evolving under* (25) *exponentially converge:*

1. *if $k_c = 0$, to formations centered at the initial center of mass, in particular:*
   - *(a) if $0 \leq |\alpha| < \pi/n$, to a single limit point;*
   - *(b) if $|\alpha| = \pi/n$, to an evenly spaced circle formation;*
   - *(c) if $\pi/n < |\alpha| < 2\pi/n$, to an evenly spaced logarithmic spiral formation;*
2. *if $k_c > 0$, to formations centered at the origin, in particular:*

(a) *if* $0 \leq |\alpha| \leq \pi/n$, *to a single limit point;*

(b) *if* $\pi/n < |\alpha| < 2\pi/n$

i. *if* $k_c > 2\sin(\pi/n)\sin(\alpha - \pi/n)$, *to a single limit point;*

ii. *if* $k_c = 2\sin(\pi/n)\sin(\alpha - \pi/n)$, *to an evenly spaced circle formation;*

iii. *if* $k_c < 2\sin(\pi/n)\sin(\alpha - \pi/n)$, *to an evenly spaced logarithmic spiral formation.*

Proof: As a consequence of Theorem IV.1, the eigenvectors of $C(\alpha)$ are linearly independent. Indeed, the eigenvectors ν_k for $k \in \{1, \ldots, 3n\}$ are linearly independent since the vectors μ_k are (see Theorem III.1); moreover, the eigenvectors ν_k for $k \in \{3n+1, \ldots, 6n\}$ are clearly linearly independent. Since, by assumption, $-k_d \notin \mathrm{eig}(A(\alpha))$, the independence of the eigenvectors of $C(\alpha)$ follows.

Then, the proof is a simple consequence of Theorem III.1, Corollary III.2, Theorem IV.1, and the arguments in Section 3.5 of.[4]

□

B. Control Law with Relative Information Only

Consider the following feedback control law:

$$\mathbf{u}_i = k_1 R^2(\alpha)\Big((\mathbf{x}_{i+2} - \mathbf{x}_{i+1}) - (\mathbf{x}_{i+1} - \mathbf{x}_i)\Big) + k_2 R(\alpha)(\dot{\mathbf{x}}_{i+1} - \dot{\mathbf{x}}_i), \tag{27}$$

where k_1 and k_2 are two real constants (not necessarily positive). In this case, each agent only needs to measure its *relative* position with respect to the positions of agents $i+1$ and $i+2$ (note that $(\mathbf{x}_{i+2} - \mathbf{x}_{i+1}) = ((\mathbf{x}_{i+2} - \mathbf{x}_i) - (\mathbf{x}_{i+1} - \mathbf{x}_i)))$, and its *relative* velocity with respect to the velocity of agent $i+1$. Note that control law (27) uses a rotation matrix that is common to all agents; hence, it requires that all agents agree upon a common orientation, but it does *not* require a consensus on a common origin. Indeed, in the case of spacecraft, agreement on the orientation can be easily achieved by using star trackers.

It is possible to verify that

$$L^2 = \begin{bmatrix} 1 & -2 & 1 & 0 & \ldots & 0 \\ 0 & 1 & -2 & 1 & \ldots & 0 \\ \vdots & & & & & \vdots \\ -2 & 1 & 0 & \ldots & \ldots & 1 \end{bmatrix}.$$

Then, the overall dynamics of the n agents can be written in compact form as

$$\begin{bmatrix} \dot{\mathbf{x}} \\ \ddot{\mathbf{x}} \end{bmatrix} = \begin{bmatrix} 0 & I_{3n} \\ k_1 L^2 \otimes R^2(\alpha) & k_2(L \otimes R(\alpha)) \end{bmatrix} \mathbf{x} \doteq F(\alpha)\,\mathbf{x}. \tag{28}$$

Let $A(\alpha) \doteq L \otimes R(\alpha)$, and define

$$\beta_{\pm} \doteq \frac{k_2}{2} \pm \sqrt{\left(\frac{k_2}{2}\right)^2 + k_1}. \tag{29}$$

The following theorem characterizes eigenvalues and eigenvectors of $F(\alpha)$.

Theorem IV.3 *Assume that $\beta_{\pm} \neq 0$. The eigenvalues of the state matrix $F(\alpha)$ in equation* (28) *are the union of:*

- *the $3n$ eigenvalues of $A(\alpha)$, each one multiplied by β_+,*
- *the $3n$ eigenvalues of $A(\alpha)$, each one multiplied by β_-.*

In other words, eig$(F(\alpha)) = \beta_+$ eig$(A(\alpha)) \cup \beta_-$ eig$(A(\alpha))$. Moreover, the eigenvector of $F(\alpha)$ corresponding to the kth eigenvalue $\lambda_k \in \beta_+$eig$(A(\alpha))$, $k \in \{1, \ldots, 3n\}$, is:

$$\nu_k \doteq \begin{bmatrix} \nu_{k,1} \\ \nu_{k,2} \end{bmatrix} = \begin{bmatrix} \mu_k \\ \lambda_k \mu_k \end{bmatrix}, \quad k \in \{1, \ldots, 3n\},$$

where μ_k is the eigenvector of $A(\alpha)$ corresponding to the eigenvalue λ_k/β_+. Similarly, the eigenvector corresponding to the kth eigenvalue $\lambda_{3n+k} \in \beta_-eig(A(\alpha))$, $k \in \{1, \ldots, 3n\}$, is:

$$\nu_{3n+k} \doteq \begin{bmatrix} \nu_{3n+k,1} \\ \nu_{3n+k,2} \end{bmatrix} = \begin{bmatrix} \mu_k \\ \lambda_k \mu_k \end{bmatrix}, \quad k \in \{1, \ldots, 3n\},$$

where μ_k is the eigenvector of $A(\alpha)$ corresponding to the eigenvalue λ_k/β_-.

Proof: First, we compute the eigenvalues of $F(\alpha)$. Note that, by the properties of the Kronecker product, $L^2 \otimes R^2(\alpha) = (L \otimes R(\alpha))^2 = A^2(\alpha)$. The eigenvalues of $F(\alpha)$ are, by definition, solutions to the characteristic equation:

$$0 = \det\left(\begin{bmatrix} \lambda I_{3n} & -I_{3n} \\ -k_1 A^2(\alpha) & \lambda I_{3n} - k_2 A(\alpha) \end{bmatrix}\right).$$

Using the result in equation (1) we have that

$$
\begin{aligned}
0 &= \det\left(\lambda^2 I_{3n} - k_2 \lambda A(\alpha) - k_1 A^2(\alpha)\right) \\
&= \det\Big((\lambda I_{3n} - \beta_+ A(\alpha))(\lambda I_{3n} - \beta_- A(\alpha))\Big).
\end{aligned}
$$

Then, the first part of the claim is proven.

By definition, the eigenvector $[\nu_{k,1}\, \nu_{k,2}]^T$ corresponding to the eigenvalue λ_k, $k \in \{1, \ldots, 6n\}$, satisfies the eigenvalue equation:

$$
\begin{aligned}
\lambda_k \begin{bmatrix} \nu_{k,1} \\ \nu_{k,2} \end{bmatrix} &= \begin{bmatrix} 0 & I_{3n} \\ k_1 A^2(\alpha) & k_2 A(\alpha) \end{bmatrix} \begin{bmatrix} \nu_{k,1} \\ \nu_{k,2} \end{bmatrix} \\
&= \begin{bmatrix} \nu_{k,2} \\ k_1 A^2(\alpha) \nu_{k,1} + k_2 A(\alpha) \nu_{k,2} \end{bmatrix}.
\end{aligned}
$$

Thus, we obtain

$$
\begin{aligned}
\lambda_k \nu_{k,1} &= \nu_{k,2}, \\
\lambda_k \nu_{k,2} &= k_1 A^2(\alpha) \nu_{k,1} + k_2 A(\alpha) \nu_{k,2},
\end{aligned}
$$

and therefore,

$$
\lambda_k^2 \nu_{k,1} = k_1 A^2(\alpha) \nu_{k,1} + k_2 A(\alpha) \lambda_k \nu_{k,1},
$$

which can be rewritten as

$$
(\lambda_k I_{3n} - \beta_+ A(\alpha))(\lambda_k I_{3n} - \beta_- A(\alpha)) \nu_{k,1} = 0. \tag{30}
$$

Therefore, if $\lambda_k \in \beta_+ \mathrm{eig} A(\alpha)$ (analogous arguments hold if $\lambda_k \in \beta_- \mathrm{eig} A(\alpha)$), the above equation is satisfied by letting $\nu_{k,1}$ be equal to μ_k, in fact in this case (notice that μ_k is the eigenvector of $A(\alpha)$ corresponding to the eigenvalue λ_k / β_+ and that $\beta_+ \neq 0$):

$$
\lambda_k \nu_{k,1} = \frac{\lambda_k}{\beta_+} \beta_+ \mu_k = \beta_+ A(\alpha) \mu_k = \beta_+ A(\alpha) \nu_{k,1},
$$

and the claim easily follows. □

By appropriately choosing k_1, k_2 and α, it is possible to obtain a variety of formations. Here we focus only on circular formations and Archimedes' spiral formations (an Archimedes' spiral is a spiral with the property that successive turnings have a constant separation distance), which are arguably among the most important symmetric formations for applications. In particular, Archimedes' spiral formations are useful for the solution of the coverage path-planning problem, where the objective is to ensure that at least one agent eventually moves to within a given distance from any point in the target environment. More applications will be discussed in Section V. We start with circular formations.

1. *Circular formations with only relative information*

We start with the following lemma.

Lemma IV.4 *The vector* $w_k = \begin{bmatrix} 0_{3n\times 1} \\ \mu_k \end{bmatrix}$, *where* $0_{3n\times 1}$ *is the zero matrix with* $3n$ *rows and* 1 *column, is a generalized eigenvector for the zero eigenvalues* λ_k, *where* $k = n, 2n, 3n$.

Proof: The claim can be easily obtained by direct verification into the equation $(F(\alpha) - \lambda_k I_{6n})w_k = \nu_k$. □

Theorem IV.5 *Let* $k_2 = 2\cos(\pi/2n)$ *and* $k_1 = -(k_2/2)^2 - \sin^2(\pi/2n)$. *Moreover, assume that* $\alpha = \pi/2n$; *then, the system converges to an evenly spaced circular formation whose geometric center has constant velocity.*

Proof: With the above choices for k_1 and k_2, it is straightforward to verify that $\beta_\pm = e^{j\pi/(2n)}$. From Theorem IV.3, $F(\alpha)$ has exactly two eigenvalues on the imaginary axis, a zero eigenvalue with algebraic multiplicity 6 and geometric multiplicity 3, and all other eigenvalues $\beta_\pm\lambda_k$ in the open left-half complex plane with linearly independent eigenvectors. Then, by using Theorem IV.3 and Lemma IV.4, it is possible to show that, as $t \to +\infty$, the time evolution of the system satisfies

$$\begin{bmatrix} \mathbf{x}(t) \\ \dot{\mathbf{x}}(t) \end{bmatrix} = \begin{bmatrix} \mathrm{x}_G \\ \dot{\mathrm{x}}_G \end{bmatrix} + t \begin{bmatrix} \dot{\mathrm{x}}_G \\ 0_{3n\times 1} \end{bmatrix} + c_1 \begin{bmatrix} \mathrm{w}^1_{dom} \\ -\omega \mathrm{w}^2_{dom} \end{bmatrix} + c_2 \begin{bmatrix} \mathrm{w}^2_{dom} \\ \omega \mathrm{w}^1_{dom} \end{bmatrix},$$

where x_G and $\dot{\mathrm{x}}_G$ are the initial position and velocity of the center of the formation, c_1 and c_2 are constants that depend on the initial conditions, ω is a constant equal to $2\sin\left(\frac{\pi}{n}\right)$, and, finally, the eigenfunctions w^p_{dom}, $p \in \{1, 2\}$, are given by:

$$\begin{aligned} \mathrm{w}^1_{dom} &= [\cos(\omega t+\delta_1), \sin(\omega t+\delta_1), 0, \ldots, \cos(\omega t+\delta_n), \sin(\omega t+\delta_n), 0], \\ \mathrm{w}^2_{dom} &= [\sin(\omega t+\delta_1), -\cos(\omega t+\delta_1), 0, \ldots, \sin(\omega t+\delta_n), -\cos(\omega t+\delta_n), 0], \end{aligned} \tag{31}$$

where $\delta_i = 2\pi(i-1)/n$, $i \in \{1, \ldots, n\}$. (Note that $\dot{\mathrm{w}}^1_{dom} = -\omega \mathrm{w}^2_{dom}$, $\dot{\mathrm{w}}^2_{dom} = \omega \mathrm{w}^1_{dom}$.) □

Next we show how to choose k_1, k_2 and α to achieve Archimedes' spiral formations; note that an Archimedes' spiral is described in polar coordinates by the equation $\varrho(\varphi) = a\varphi$, with $a \in \mathbb{R}_{>0}$.

2. Archimedes' spiral formations with only relative information

We start with the following lemma.

Lemma IV.6 *Let $k_1 = -(k_2/2)^2$ and assume $\alpha = \pi/n$. Then, $w_k = \begin{bmatrix} 0_{3n\times 1} \\ \mu_k \end{bmatrix}$ is a generalized eigenvector for the eigenvalue λ_k/β.*

Proof: The claim can be easily obtained by direct verification into the equation $(F(\alpha) - \lambda_k I_{6n})w_k = \nu_k$. □

Theorem IV.7 *Let $k_1 = -(k_2/2)^2$, and assume $k_2 > 0$ and $\alpha = \pi/n$. Then, the system converges to an Archimedes' spiral formation whose geometric center has constant velocity.*

Proof: In this case we have $\beta_+ = \beta_- \in \mathbb{R}_{>0}$, and thus $\lambda_k = \lambda_{k+3n}$ for all $k \in \{1, \ldots, 3n\}$; as a consequence, the eigenvalues of $F(\alpha)$ are $\beta\,\mathrm{eig}(A(\alpha))$. Hence, $F(\alpha)$ has exactly two eigenvalues on the imaginary axis, each one with algebraic multiplicity 2 and geometric multiplicity 1, a zero eigenvalue with algebraic multiplicity 6 and geometric multiplicity 3, and all other eigenvalues $\beta_\pm \lambda_k$ in the open left-half complex plane. Then, by using Theorem IV.3 and Lemma IV.6, it is possible to show that, as $t \to +\infty$, the time evolution of the system satisfies

$$\begin{bmatrix} \mathbf{x}(t) \\ \dot{\mathbf{x}}(t) \end{bmatrix} = \begin{bmatrix} \mathrm{x}_G \\ \dot{\mathrm{x}}_G \end{bmatrix} + t \begin{bmatrix} \dot{\mathrm{x}}_G \\ 0_{3n\times 1} \end{bmatrix} + d_1 \begin{bmatrix} 0_{3n\times 1} \\ \mathrm{w}^1_{dom} \end{bmatrix} + d_2 \begin{bmatrix} 0_{3n\times 1} \\ \mathrm{w}^2_{dom} \end{bmatrix}$$
$$+ (c_1 + d_1 t) \begin{bmatrix} \mathrm{w}^1_{dom} \\ -\omega \mathrm{w}^2_{dom} \end{bmatrix} + (c_2 + d_2 t) \begin{bmatrix} \mathrm{w}^2_{dom} \\ \omega \mathrm{w}^1_{dom} \end{bmatrix},$$

where x_G and $\dot{\mathrm{x}}_G$ are the initial position and velocity of the center of the formation, c_1, c_2, d_1 and d_2 are constants that depend on the initial conditions, ω is a constant equal to $2\sin\left(\frac{\pi}{n}\right)$, and, finally, the eigenfunctions w^p_{dom}, $p \in \{1, 2\}$, are defined in equation (31). Then, agents will perform spiraling trajectories; the radial growth rate is a constant equal to $\sqrt{d_1 + d_2}$, and the center of the formation moves with constant velocity $\dot{\mathbf{x}}_G$ defined by the initial conditions. □

C. Comparison with existing results in the literature

It is of interest to discuss the relation between the control policies presented so far and a set of related results recently appeared in.[15,16] First, in,[15] Ren proposes the following control law for the single-integrator model in equation (7):

$$\mathbf{u}_i = -\sum_{k=1}^{n} q_{ik} R(\alpha)(\mathbf{x}_i - \mathbf{x}_k), \quad i \in \{1, \ldots, n\},$$

where q_{ik} is the (i,k)th entry of a weighted adjacency matrix Q associated to a weighted directed graph $\mathcal{G}$ (notice that the ring topology is a special case). In,[15] it is shown that if $\mathcal{G}$ has a directed spanning tree, the agents will eventually converge to a single point, a circle or a logarithmic spiral pattern, depending on the value of α; the center of the formation is determined by the initial positions, and the circular formation, whose radius is determined by the initial positions, is achieved when certain eigenvalues are on the imaginary axis. Our results in Section III differ from the results in[15] along two main dimensions: (i) we consider control on the center of the formation; (ii) most importantly, we consider the problem of *robust* convergence to a circular motion on a circle of *prescribed* radius (see Section III.B).

Second, in,[16] Ren proposes the following control law for the double-integrator model in equation (23):

$$\mathbf{u}_i = -\sum_{k=1}^{n} q_{ik} R(\alpha)(\mathbf{x}_i - \mathbf{x}_k) - \gamma\, \dot{\mathbf{x}}_i, \quad i \in \{1, \ldots, n\}, \gamma \in \mathbb{R}_{>0},$$

where q_{ik} is, as before, the (i,k)th entry of a weighted adjacency matrix Q associated to a weighted directed graph $\mathcal{G}$. In,[16] it is shown that if $\mathcal{G}$ has a directed spanning tree, the agents will eventually converge to a single point, a circle or a logarithmic spiral pattern, depending on the value of α; the center of the formation is determined by the initial conditions and the velocity needs to be measured in a common frame of reference. Our results in Section IV differ from the results in[16] along three main dimensions: (i) we consider control on the center of the formation; (ii) we study control laws that only require relative measurements of position and velocity; (iii) we consider a novel type of symmetric formation, namely Archimedes' spirals.

We next describe possible applications for the control laws we proposed, and we present experimental results.

V. Applications of Cyclic-Pursuit Algorithms

In the past few years, cyclic pursuit has received considerable attention in the control community (see Section I); however to date, to the best of our knowledge, no application has been proposed for which cyclic pursuit is a particularly effective control strategy. In this section, we discuss application domains in which cyclic pursuit is indeed an ideal candidate control law.

A. Interferometric Imaging in Deep Space

Interferometric imaging, i.e., image reconstruction from interferometric patterns, is an application of formation flight that has been devised and studied for space missions such as NASA's TPF and ESA's Darwin.[2] The general problem of interferometric imaging consists of performing measurements in a way that enough information about the frequency content of the image is obtained. Such coverage problem is independent of the global positions of the spacecraft;[3] additionally, missions like TPF and Darwin consider locations far out of the reach of GPS signals and are expected to only rely on relative measurements to perform reconfigurations and observation maneuvers. Finally, a heuristic solution to this problem is represented by *Archimedes' spiral* trajectories .[3] Hence, the application of the cyclic-pursuit algorithms presented in Section IV is inherently appropriate in this context. Figure 2 shows simulated trajectories resulting from the application of control law (27); the initial positions are random inside a volume of $(10km)^3$. In the first case spacecraft converge to circular trajectories, while in the second case spacecraft converge to Archimedes' spirals. The inertial frame for the plots is the geometric center of the configuration.

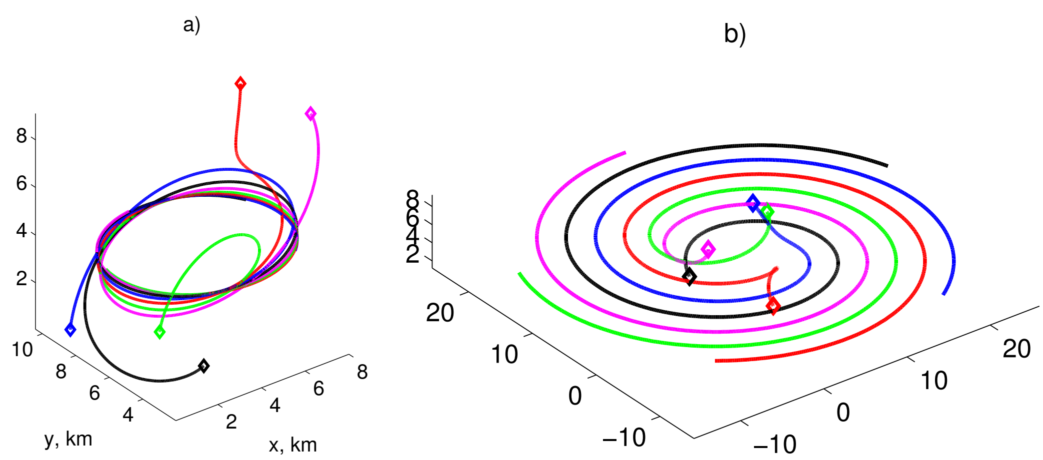

Figure 2. Convergence from random initial conditions to symmetric formations. Left Figure: Circular trajectories. Right Figure: Archimedes' spiral trajectories.

B. On Reaching Natural Trajectories

In this section we modify the previous control laws to achieve convergence to elliptical trajectories. Consider the application of a similarity transformation to the rotation matrix $R(\alpha)$, in other words, we now replace the rotation matrix $R(\alpha)$ in the previous control laws with $TR(\alpha)T^{-1}$, where T is a non-singular matrix. Such similarity transformation does not change the eigenvalues of $L \otimes R(\alpha)$ (hence Theorem III.1 still holds), but changes the eigenvectors μ of $R(\alpha)$ to $T\mu$. It is straightforward to see that the trajectories arising with the previous control laws are then transformed according to

$$\tilde{\mathbf{x}}_i(t) \;=\; T\mathbf{x}_i(t), \quad i \in \{1, \ldots, n\}; \tag{32}$$

in particular, circular trajectories can be transformed into *elliptical* trajectories.

Indeed, the above approach is useful to allow the system to globally converge to low-effort trajectories. Consider the dynamic system

$$\begin{aligned} \ddot{\mathbf{x}}_i &= f(\mathbf{x}_i, \dot{\mathbf{x}}_i) + \mathbf{u}_i \\ &= f(\mathbf{x}_i, \dot{\mathbf{x}}_i) - (f(\mathbf{x}_i, \dot{\mathbf{x}}_i) - \mathbf{u}_{nom_i}), \end{aligned} \tag{33}$$

which has a zero-effort ($\mathbf{u}_i$=0) invariant set $\mathbf{x}_i^*$, for which $f(\mathbf{x}_i^*, \dot{\mathbf{x}}_i^*) = \mathbf{u}_{nom_i}$. If we use a controller for which the state reaches $\mathbf{x}_i^*(t)$ as $t \to \infty$, then the control effort will tend to $\mathbf{u}_i = 0$ as $t \to \infty$.

In the case of the dynamics of relative orbits slightly perturbed from a circular orbit, elliptical relative trajectories are closed near-natural trajectories (i.e. theoretically they require no control effort); in the following section, cyclic-pursuit controllers are proposed as promising algorithms for formation acquisition, maintenance and reconfiguration.

1. Clohessy-Wiltshire model

The Clohessy-Wiltshire model approximates the motion of a spacecraft with respect to a frame that follows a circular orbit with angular velocity ω_R and radius $R_{ref} = (\mu_\oplus/\omega_R^2)^{1/3}$, where $\mu_\oplus$ is the gravitational constant of earth. The equations of motion $\ddot{\mathbf{x}}_i = f(\mathbf{x}_i, \mathbf{u}_i)$ are:

$$\begin{aligned} \ddot{x}_i &= 2\omega_R \dot{y}_i + 3\omega_R^2 x_i + u_{ix}, \\ \ddot{y}_i &= -2\omega_R \dot{x}_i + u_{iy}, \\ \ddot{z}_i &= -\omega_R^2 z_i + u_{iz}, \end{aligned} \tag{34}$$

where the x, y and z coordinates are expressed in a right-handed orthogonal reference frame such that the x-axis is aligned with the radial vector of the reference orbit, the z-axis is aligned with the angular momentum vector of the reference orbit, and the y-axis completes the right-handed orthogonal frame.

Consider a formation of spacecraft that use the cyclic-pursuit controller

$$\begin{aligned}\mathbf{u}_i = -f(\mathbf{x}_i) + k_g(k_d T R(\alpha) T^{-1}(\mathbf{x}_{i+1} - \mathbf{x}_i) + T R(\alpha) T^{-1}(\dot{\mathbf{x}}_{i+1} - \dot{\mathbf{x}}_i) \\ - k_c k_d \mathbf{x}_i - (k_c + k_d/k_g)\dot{\mathbf{x}}_i),\end{aligned} \tag{35}$$

with $k_g = \omega_R/(2\sin(\pi/n))$, and

$$T = \begin{bmatrix} \frac{1}{2} & 0 & 0 \\ 0 & 1 & 0 \\ z_0\cos(\phi_z) & z_0\sin(\phi_z) & 1 \end{bmatrix},$$

where z_0 and ϕ_z are tunable parameters (their roles will become clear later). Then, from the results in Section IV, we obtain, as $t \to \infty$,

$$\mathbf{x}_i(t) = \mathbf{x}_i^*(t) = T \begin{bmatrix} r\sin(\omega_R t + \delta_i) \\ r\cos(\omega_R t + \delta_i) \\ 0 \end{bmatrix}, \quad i \in \{1, \ldots, n\},$$

where $\delta_i = 2\pi(i-1)/n$, and r is a constant that depends on the initial conditions. Thus, we obtain

$$\begin{aligned} x_i^*(t) &= \frac{1}{2} r\sin(\omega_R t + \delta_i), \\ y_i^*(t) &= r\cos(\omega_R t + \delta_i), \\ z_i^*(t) &= z_o r\sin(\omega_R t + \delta_i + \phi_z); \end{aligned}$$

hence, the formation will converge to an evenly-spaced elliptical formation with an $x:y$ ratio equal to $1:2$, a $y:z$ ratio equal to $1:z_0$, and a phasing between the x and z motion equal to ϕ_z. By replacing these equations into equation (34), it is easily shown that as $\mathbf{x}(t) \to \mathbf{x}^*(t)$, we have $\mathbf{u} \to 0$.

2. Including J_2 perturbation

A more accurate model for the motion of a spacecraft considers the effects of the J_2 gravitational term. In,[5] the authors show that the equations of motion relative to a circular non-keplerian reference orbit and including the J_2 term are well approximated by the linear system:

$$
\begin{aligned}
\ddot{x}_i &= 2\omega_R c\dot{y}_i + (5c^2-2)\omega_R^2 x_i + u_{xi} + \frac{3}{4}K_{J2}\cos(2\bar{k}t),\\
\ddot{y}_i &= -2\omega_R c\dot{x}_i + u_{yi} + \frac{1}{2}K_{J2}\sin(2\bar{k}t),\\
\ddot{z}_i &= -q^2 z_i + 2lq\cos(qt+\Phi) + u_{zi},
\end{aligned}
$$

where, again, the x, y and z coordinates are expressed in a right-handed orthogonal reference frame such that the x-axis is aligned with the radial vector of the reference orbit, the z-axis is aligned with the angular momentum vector of the reference orbit, and the y-axis completes the right-handed orthogonal frame; moreover, $c = \sqrt{1+s}$, $s = \frac{3J_2R_e^2}{8r_{ref}^2}(1+3\cos(2i_{ref}))$, $K_{J2} = \frac{3\omega_R^2 J_2 R_e^2}{r_{ref}}\sin^2(i_{ref})$, R_e is the nominal radius of the earth, $\bar{k} = c + \frac{3J_2R_e^2}{2r_{ref}^2}\cos^2 i_{ref}$, r_{ref} and i_{ref} are parameters of the reference orbit, q is approximately equal to $c\omega_R$, and Φ, l are time varying functions of the difference in orbit inclination (see ref.[5] for the details). Zero-effort trajectories (i.e, trajectories with $\mathbf{u}_i = 0$) for the above dynamic model are shown to be:

$$
\begin{aligned}
x^*(t) &= x_0\cos(\omega_R t\sqrt{1-s}) + \frac{\sqrt{1-s}}{2\sqrt{1+s}}y_0\sin(\omega_R t\sqrt{1-s}) + x_{cc}(t),\\
y^*(t) &= x_0\frac{-2\sqrt{1+s}}{\sqrt{1-s}}\sin(\omega_R t\sqrt{1-s}) + y_0\cos(\omega_R t\sqrt{1-s}) + y_{cc}(t),\\
z^*(t) &= (lt+m)\sin(qt+\Phi),
\end{aligned}
\tag{36}
$$

with

$$
\mathbf{x}_{cc}(t) = [\alpha(\cos(2\bar{k}t) - \cos(\omega_R t\sqrt{1-s})),\ \beta\sin(2\bar{k}t) - \frac{2\sqrt{1+s}}{\sqrt{1-s}}\alpha(\cos(\omega_R t\sqrt{1-s})),\ 0]^T,
$$

where α, β, and m are constants that depend on the reference orbit parameters and for brevity are not discussed here. (For details we refer the reader to the work of Schweigart and Sedwick.[5]) As in the previous section, by defining the control coordinates in a reference frame centered in $\mathbf{x}_{cc}(t)$, and using the decentralized cyclic-pursuit controller in equation (35) with a transformation matrix

$$
T = \begin{bmatrix} \frac{\sqrt{1-s}}{2\sqrt{1+s}} & 0 & 0\\ 0 & 1 & 0\\ z_0\cos(\phi_z) & z_0\sin(\phi_z) & 1 \end{bmatrix},
$$

and $k_g = \omega_R\sqrt{1-s}/(2\sin(\pi/n))$, it is straighforward to show that the formation will converge to elliptical trajectories centered at the point $\mathbf{x}_{cc}(t)$. Then, as $t \to \infty$, $\mathbf{x}(t) \to$

$T\begin{bmatrix} r\sin(\omega_R t+\delta_i) \\ r\cos(\omega_R t+\delta_i) \\ 0 \end{bmatrix} + \mathbf{x}_{cc}$, and thus, as $t \to \infty$, the trajectories for $x(t)$, $y(t)$ are those described in equation (36), and we have that:

$$
\begin{aligned}
u_x &\to 0, \\
u_y &\to 0, \\
u_z &\to (\omega_R^2 - q^2) + 2lq\cos(qt+\Phi) \approx 2lq\cos(qt+\Phi).
\end{aligned}
$$

The last term corresponds to the cohesive force required to maintain the formation when the orbits are not coplanar (i.e. the spacecraft have different inclination and thus different J_2 secular drift rates). For $z_o \to 0$, then $q = \omega_R$, $l \to 0$ and the theoretical required thrust converges to zero.

Figure 3 shows simulation results for the control laws described in this section. The system is simulated using dynamics including the J_2 terms. The results show convergence from random initial positions to the desired orbits, i.e., an evenly-spaced elliptical formation in the desired plane. It is also shown (Fig. 3b) how the control effort reduces as the spacecraft reach the desired low-effort trajectories.

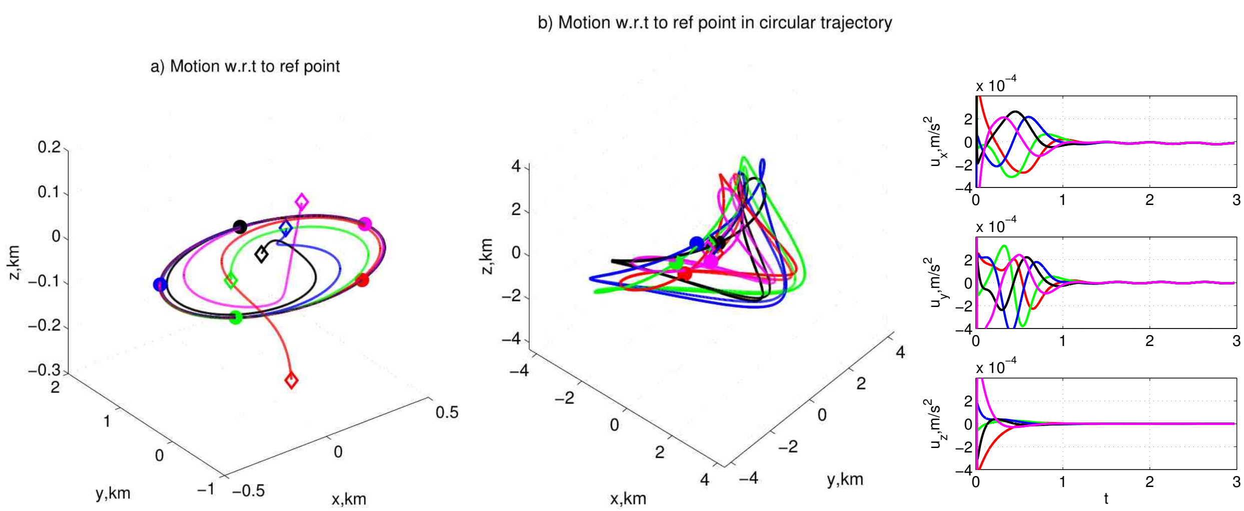

Figure 3. Convergence to elliptical trajectories with dynamics including J_2 terms. The dots indicate the positions after 3 orbits. Left Figure: 3D view, trajectories with respect to reference point $\mathbf{x}_{cc}$. Center Figure: 3D view, trajectories with respect to non-keplerian circular orbit. Right Figure: Control effort versus time; note that as $t \to \infty$, $\mathbf{u} \to 0$.

Although the achieved trajectories are not natural trajectories for a free orbiting body, the proposed decentralized control law allows convergence to elliptical formations that are near-natural and would require low fuel consumption for their maintenance.

VI. Experimental Results on a Microgravity Environment

The previous control laws have been tested on the SPHERES testbed on board the International Space Station. SPHERES is an experimental testbed consisting of a group of small vehicles with the basic functionalities of a satellite.[21] Their propulsion system uses compressed CO_2 gas, and their metrology system is "GPS-like". Each vehicle has a local estimator that calculates a global estimate of the state from measurements of ultrasound pulses. The system uses a single TDMA based RF channel to communicate its state to neighboring spacecraft. Figure 4 shows a picture of three SPHERES spacecraft on board the ISS.

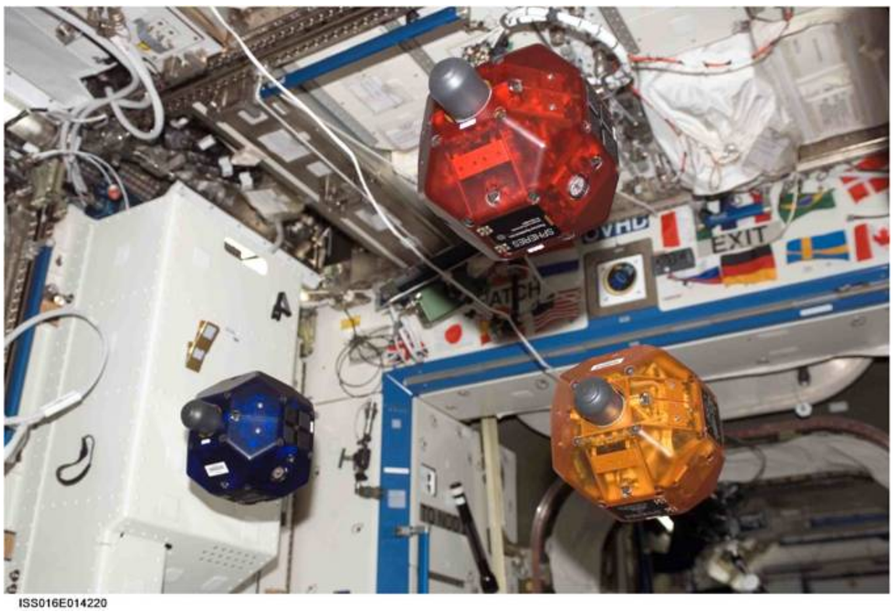

Figure 4. Picture of three SPHERES satellites performing a test on board the ISS. (Fotocredit: NASA - SPHERES)

The dynamics of each spacecraft are well approximated by a double integrator. For the tests presented in this section, we used a velocity-tracking control law to track the velocity profile in equation (16). We set $k_\alpha = 1$, while the gain k_g (and consequently the frequency of rotation) was set in each maneuver to make the centripetal force for the circular motion equal to $0.11N$ (half the saturation level of the thrusters). We next describe two tests performed using the SPHERES testbed on board the ISS: the objective is to demonstrate the closed-loop robustness of the approach.

A. Test 1

The first test comprised the following series of maneuvers, with the initial conditions being $x_1 = [0, -0.1, -0.2]^T$, $x_2 = [0, 0.1, 0.2]^T$, $x_3 = [0, 4, 0]^T$ and zero velocity (with respect to the ISS):

a) two spacecraft perform a rotation maneuver in the x-z plane with a radius $r = 0.3m$;

b) a change in the desired radius is commanded and the spacecraft spiral out to achieve a circular formation with $r = 0.4m$;

c) a third spacecraft joins the formation and the system reconfigures into a three-spacecraft evenly-spaced circular formation with $r = 0.35m$;

d) a similarity transformation T is applied to the rotation matrix, and the spacecraft achieve an elliptical formation with eccentricity equal to 0.8.

The objective was to test convergence to evenly-spaced circular formations and robustness with respect to changes in the number of agents. Figure 5 shows global position and velocity of each spacecraft (with respect to the ISS); figure 6 shows the trajectories performed by the spacecraft during the maneuvers a), b), c) and d). Experimental results (see in particular Fig. 6) demonstrate the effectiveness of the proposed cyclic-pursuit controller.

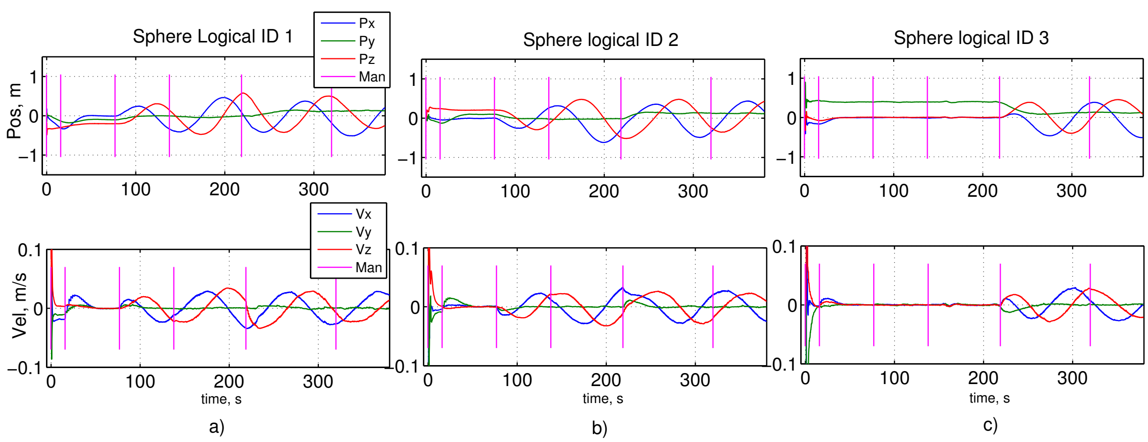

Figure 5. Experimental results from Test 1: Position and velocity vs. time. From left to right: satellites 1, 2 and 3.

B. Test 2

The second test comprised the following series of maneuvers, with the initial conditions being $x_1 = [0, -0.1, -0.2]^T$, $x_2 = [0, 0.1, 0.2]^T$, $x_3 = [0, 4, 0]^T$ and zero velocity (with respect to the ISS):

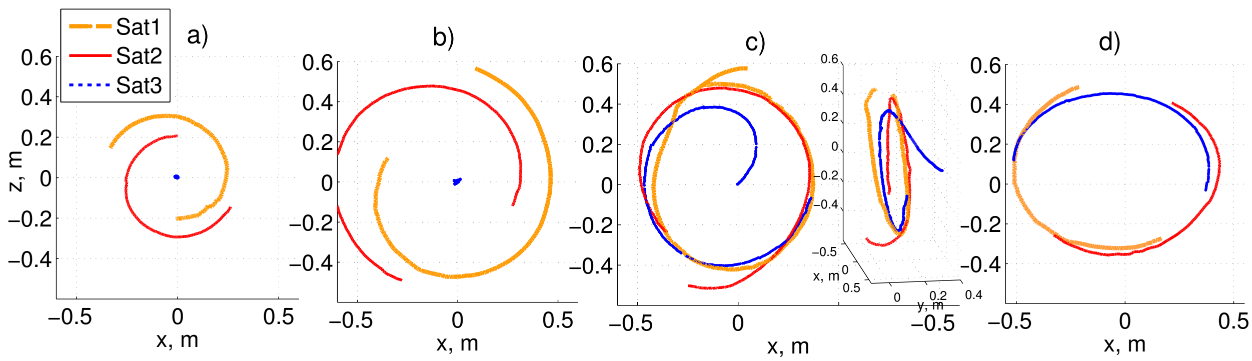

Figure 6. Experimental results from Test 1: x-z plane. Sequence of maneuvers a), b), c) and d).

a) three spacecraft perform an evenly-spaced rotation maneuver in the x-z plane with radius $r = 0.35m$;

b) a similarity transformation T is applied to the rotation matrix, and the spacecraft achieve an elliptical formation with eccentricity equal to 0.8.

Figure 7 shows global position and velocity of each spacecraft (with respect to the ISS); figure 8 shows the trajectories performed by the spacecraft during the maneuvers a) and b). Also in this case, experimental results (see in particular Fig. 8) demonstrate the effectiveness of the proposed cyclic-pursuit controller. Videos of experimental results can be accessed at http://ssl.mit.edu/spheres/video/CyclicPursuit.

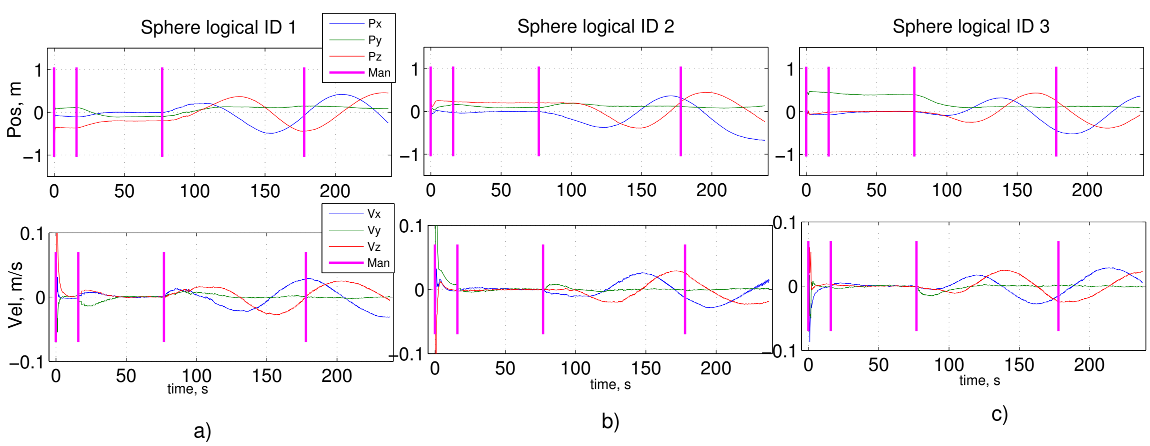

Figure 7. Experimental results from Test 2: Position and velocity vs. time. From left to right: satellites 1, 2 and 3.

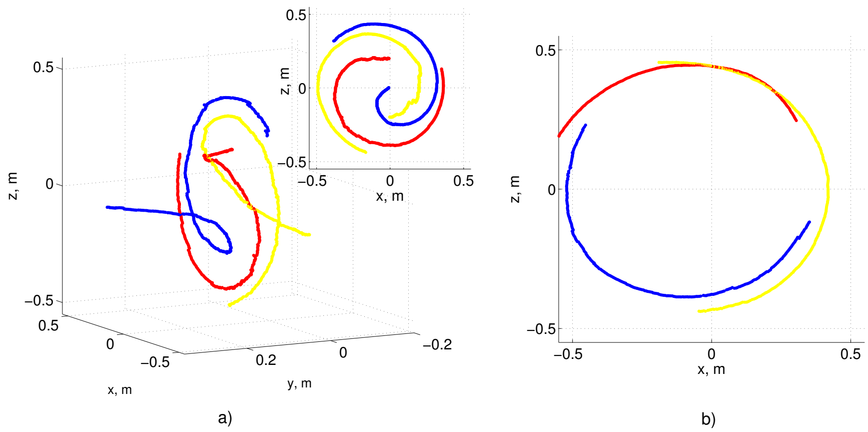

Figure 8. Experimental results from Test 2: x-z plane. Sequence of maneuvers a) and b).

VII. Conclusions

In this paper we studied distributed control policies for spacecraft formation that draw inspiration from the simple idea of cyclic pursuit. We discussed potential applications and we presented experimental results. This paper leaves numerous important extensions open for further research. First, all of the algorithms that we proposed are synchronous: we plan to devise algorithms that are amenable to asynchronous implementation. Second, we envision to study the problem of convergence to symmetric formations in presence of actuator saturation. Finally, to further assess closed-loop robustness, we plan to perform additional tests on board the ISS.

Acknowledgements

The authors would like to thank the SPHERES team at the Space Systems Laboratory at MIT, especially Dr. Alvar Sanz-Otero and Christopher Mandy, for facilitating the implementation on board the ISS and for their support in obtaining the experimental results.

This work was supported in part by NSF grants #0705451 and #0705453. Any opinions, findings, and conclusions or recommendations expressed in this publication are those of the authors and do not necessarily reflect the views of the supporting organizations.

Appendix

A. System (18) in Polar Coordinates

Assume that $\|\mathbf{p}_i\| = \varrho_i > 0$. Note that $\mathbf{p}_i = \varrho_i R(-\vartheta_i)\, e_1$, where e_1 is the first vector of the canonical basis, i.e., $e_1 = (1,\, 0)^T$. Then, we can write $\mathbf{p}_{i+1}$ as

$$\mathbf{p}_{i+1} = \frac{\varrho_{i+1}}{\varrho_i}\varrho_i R(-\vartheta_{i+1})\, e_1 = \frac{\varrho_{i+1}}{\varrho_i}\varrho_i R(-\vartheta_{i+1}) R(\vartheta_i) R(-\vartheta_i)\, e_1 = \frac{\varrho_{i+1}}{\varrho_i} R(\vartheta_i - \vartheta_{i+1})\,\mathbf{p}_i. \quad (37)$$

Moreover, it also holds

$$\mathbf{p}_i^T R(\gamma) p_i = \|\mathbf{p}_i\|^2 \cos(\gamma) = \varrho_i^2 \cos(\gamma), \quad \text{for any} \quad \gamma \in \mathbb{R}. \quad (38)$$

First, we find the differential evolution for the magnitude of $\mathbf{p}_i$, i.e., for ϱ_i. We have

$$\dot{\varrho}_i = \frac{d\|\mathbf{p}_i\|}{dt} = \frac{\mathbf{p}_i^T \dot{\mathbf{p}}_i}{\|\mathbf{p}_i\|} = \frac{1}{\varrho_i}\,\mathbf{p}_i^T (R(\alpha_{i+1})\mathbf{p}_{i+1} - R(\alpha_i)\mathbf{p}_i).$$

By using Eqs. (37) and (38) we then obtain

$$\dot{\varrho}_i = \frac{1}{\varrho_i}\,\mathbf{p}_i^T \Big(R(\alpha_{i+1}) \frac{\varrho_{i+1}}{\varrho_i} R(\vartheta_i - \vartheta_{i+1})\,\mathbf{p}_i - R(\alpha_i)\mathbf{p}_i \Big) = \varrho_i \cos((\vartheta_{i+1} - \vartheta_i) - \alpha_{i+1}) - \varrho_i \cos(\alpha_i).$$

We now find the differential evolution for the phase of $\mathbf{p}_i$, i.e., for ϑ_i. Taking time derivative in both hands of the identity $p_{i,1} \sin \vartheta_i - p_{i,2} \cos \vartheta_i = 0$, we easily obtain

$$\dot{\vartheta}_i = \frac{p_{i,1}\,\dot{p}_{i,2} - p_{i,2}\,\dot{p}_{i,1}}{\varrho_i^2} = \frac{1}{\varrho_i^2}\mathbf{p}_i^T R\Big(\frac{\pi}{2}\Big)\dot{\mathbf{p}}_i = \frac{1}{\varrho_i^2}\mathbf{p}_i^T R\Big(\frac{\pi}{2}\Big)\Big(R(\alpha_{i+1})\mathbf{p}_{i+1} - R(\alpha_i)\mathbf{p}_i\Big).$$

Then, by using Eqs. (37) and (38) we obtain

$$\dot{\vartheta}_i = \frac{1}{\varrho_i^2}\mathbf{p}_i^T R\Big(\frac{\pi}{2}\Big)\Big(R(\alpha_{i+1})\frac{\varrho_{i+1}}{\varrho_i} R(\vartheta_i - \vartheta_{i+1})\,\mathbf{p}_i - R(\alpha_i)\mathbf{p}_i\Big) = \frac{\varrho_{i+1}}{\varrho_i}\,\sin((\vartheta_{i+1} - \vartheta_i) - \alpha_{i+1}) + \sin(\alpha_i).$$

B. Proof of Lemma III.8

Proof: The eigenvalues of P are solutions to the characteristic equation

$$0 = \det\left(\begin{bmatrix} \lambda I_n - a_n\, L + 2k_\alpha\, s_n\, I_n & s_n\, I_n \\ -b_n\, L^2 & \lambda I_n - c_n\, L \end{bmatrix}\right).$$

Note that both matrix $(\lambda I_n - a_n\, L + 2k_\alpha\, s_n\, I_n)$ and matrix $-b_n\, L^2$ are circulant; then, since circulant matrices form a commutative algebra (see Section II), we can apply the result in equation (1) and obtain

$$
\begin{aligned}
0 &= \det\Big((\lambda I_n - a_n\, L + 2k_\alpha\, s_n I_n)(\lambda I_n - c_n\, L) + s_n b_n L^2\Big) \\
&= \det\Bigg(\lambda^2 I_n + \lambda\Big(\underbrace{2k_\alpha\, s_n I_n - (a_n + c_n)L}_{\doteq B}\Big)\, \underbrace{-2k_\alpha s_n c_n L + (a_n c_n + s_n b_n)L^2}_{\doteq C}\Bigg) \\
&= \det\Big(\lambda^2 I_n + \lambda B + C\Big) \\
&= \det\Big(\lambda^2 I_n + \lambda B + B^2/4 - S\Big),
\end{aligned}
$$

where $S \doteq B^2/4 - C$. Note that B and C are circulant, therefore S is also circulant. Since S is circulant, it can be diagonalized according to $S = U\, D_S\, U^*$, where D_S is a diagonal matrix with the eigenvalues of S on the diagonal; accordingly, we have $S^{1/2} = U\, D_S^{1/2}\, U^*$. Note that B and $S^{1/2}$ commute. In fact, since B is circulant, it can be diagonalized via the same orthogonal matrix U: $B = U\, D_B U^*$, where D_B is a diagonal matrix with the eigenvalues of B on the diagonal; hence

$$
S^{1/2}\, B = U D_S^{1/2} U^*\, U D_B U^* = U D_S^{1/2} D_B U^* = U D_B D_S^{1/2} U^* = U D_B U^*\, U D_S^{1/2} U^* = B\, S^{1/2}.
$$

Therefore, we have

$$
0 = \det\Big(\lambda^2 I_{n\times n} + \lambda B + B^2/4 - S\Big) = \det\Big(\lambda I_n - (-B/2 + \sqrt{S})\Big)\det\Big(\lambda I_{n\times n} - (-B/2 - \sqrt{S})\Big).
$$

Hence, the eigenvalues of P are the union of the eigenvalues of $(-B/2 + \sqrt{S})$ and $(-B/2 - \sqrt{S})$. Since B and $S^{1/2}$ are diagonalized by the same similarity transformation U, we have

$$
-\frac{B}{2} \pm S^{1/2} = U\frac{D_B}{2}U^* \pm U D_S^{1/2} U^* = U\left(\frac{D_B}{2} \pm D_S^{1/2}\right)U^*. \tag{39}
$$

Let $\lambda_{B,k}$ be the kth eigenvalue of B, and $\lambda_{S,k}$ be the kth eigenvalue of S, $k \in \{1, \ldots, n\}$. Then, from equation (39), we have that

$$
\mathrm{eig}(P) = \left\{\lambda_{B,k}/2 \pm \lambda_{S,k}^{1/2}\right\}_{k=1}^{n}.
$$

Hence, we are left with the task of computing the eigenvalues of B and S. Such eigenvalues can be easily found by using equation (4):

$$\begin{aligned}
\mathrm{eig}(B) &= \left\{2k_\alpha\, s_n + (a_n + c_n)(1 - e^{2\pi jk/n})\right\}_{k=1}^{n}, \\
\mathrm{eig}(S) &= \left\{(\lambda_{B,k}^2/4 - \lambda_{C,k}\right\}_{k=1}^{n} = \left\{(2k_\alpha\, s_n + (a_n + c_n)(1 - e^{2\pi jk/n})^2/4\right. \\
&- \Big((2k_\alpha s_n c_n + a_n c_n + s_n b_n) - (2k_\alpha s_n c_n + 2a_n c_n + 2s_n b_n)e^{2\pi jk/n} \\
&+ \left.(a_n c_n + b_n s_n)e^{4\pi jk/n}\Big)\right\}_{k=1}^{n}.
\end{aligned}$$

We first consider the eigenvalues of B. By using the following identities

$$(1 - e^{\alpha_k} j) = 2\sin(\alpha_k/2)e^{j\frac{\alpha_k - \pi}{2}}, \qquad (1 - \frac{1}{2}(1 - e^{j\alpha_k})) = \cos(\alpha_k/2)e^{j\alpha_k/2}, \tag{40}$$

and after some algebraic manipulations omitted for brevity, the eigenvalues of B can be written as

$$\lambda_{B,k} = (2k_\alpha s_n) + 2(2c_n - k_\alpha s_n)\sin(k\pi/n)e^{j(k\pi/n - \frac{\pi}{2})}, \quad k \in \{1, \ldots, n\}. \tag{41}$$

Hence, we have, for $k \in \{1, \ldots, n\}$,

$$\begin{aligned}
Re(\lambda_{B,k}) &= 2k_\alpha s_n + 2(2c_n - k_\alpha s_n)\sin^2(k\pi/n), \\
Im(\lambda_{B,k}) &= -2(2c_n - k_\alpha s_n)\sin(k\pi/n)\cos(k\pi/n).
\end{aligned} \tag{42}$$

Next, we consider the eigenvalues of S. By using, again, the identities in equation (40), and with simple algebraic manipulations, we can write, for $k \in \{1, \ldots, n\}$,

$$\begin{aligned}
\lambda_{S,k} &= k_\alpha^2 s_n^2(\cos(k\pi/n)e^{jk\pi/n})^2 + (k_\alpha s_n c_n + s_n^2)(2\sin(k\pi/n)e^{j(k\pi/n - \frac{\pi}{2})})^2 \\
&= [k_\alpha^2 s_n^2 + 4\sin^2(k\pi/n) + (4k_\alpha s_n c_n - k_\alpha^2 s_n^2 - 4c_n^2)\sin^2(k\pi/n)]e^{i2k\pi/n}.
\end{aligned}$$

Notice that k_α, c_n and s_n are positive real numbers; then the term inside the square brackets is a positive real number. Therefore we have, for $k \in \{1, \ldots, n\}$,

$$Re(\sqrt{\lambda_{S,k}}) = (k_\alpha^2 s_n^2 + 4\sin^2(k\pi/n) + (4k_\alpha s_n c_n - k_\alpha^2 s_n^2 - 4c^2)(\sin^2(k\pi/n)))^{1/2}\cos(k\pi/n),$$

which can be rearranged as

$$\begin{aligned}
Re(\sqrt{\lambda_{S,k}}) &= \left((k_\alpha s_n + (2c_n - k_\alpha s_n)\sin^2(k\pi/n))^2 + 4\sin^2(k\pi/n)(s_n^2 - \sin^2(k\pi/n))\right)^{1/2} \\
&= \left((\lambda_{B,1}/2)^2 + 4\sin^2(k\pi/n)(s_n^2 - \sin^2(k\pi/n))\right)^{1/2}.
\end{aligned} \tag{43}$$

From equations (42) and (43) it is straigthforward to show that

- For $k = n$: we have

$$\lambda_{P,n} = -\lambda_{B,n}/2 + \sqrt{\lambda_{S,n}} = k_\alpha s_n - k_\alpha s_n = 0.$$

- For $k = 1$, $k = n - 1$:

$$\begin{aligned} Re(\sqrt{\lambda_{S,1}}) &= Re(\lambda_{B,1}/2) = (k_\alpha s_n c_n^2 + 2s_n^2 c_n), & Im(\sqrt{\lambda_{S,1}}) &= k_\alpha s_n^2 c_n + 2s_n^3, \\ Re(\sqrt{\lambda_{S,n-1}}) &= Re(\lambda_{B,n-1}/2) = (k_\alpha s_n c_n^2 + 2s_n^2 c_n), & Im(\sqrt{\lambda_{S,n-1}}) &= -k_\alpha s_n^2 c_n - 2s_n^3. \end{aligned}$$

  Therefore, we obtain

$$\begin{aligned} Re(\lambda_{P,1}) &= -Re(\lambda_{B,1}/2) + Re(\lambda_{B,1}/2) = 0, \\ Im(\lambda_{P,1}) &= (2c_n - k_\alpha s_n) s_n c_n + k_\alpha s_n^2 c_n + 2s_n^3 = 2s_n, \\ Re(\lambda_{P,n-1}) &= -Re(\lambda_{B,n-1}/2) + Re(\lambda_{B,n-1}/2) = 0, \\ Im(\lambda_{P,n-1}) &= -(2c_n - k_\alpha s_n) s_n c_n - k_\alpha s_n^2 c_n + 2s_n^3 = -2s_n. \end{aligned}$$

- For $1 < k < n - 1$, since $\sin(k\pi/n)^2 > \sin(\pi/n)^2$, we have:

$$Re(\sqrt{\lambda_{S,k}}) \leq Re(\lambda_{B,k}/2),$$

  and thus $Re(\lambda_{P,k}) < 0$ for $k \notin \{0, 1, n-1\}$.

Now, we proceed to show that v_1, v_2, v_3 in lemma III.8 are the eigenvectors corresponding to the eigenvalues 0, $2s_n j$ and $-2s_n j$ respectively. First, consider the zero eigenvalue. Since $L \cdot \mathbf{1}_n = \mathbf{0}_n$ (where $\mathbf{0}_n = (0, 0, \ldots, 0)^T \in \mathbb{R}^n$), it is easy to verify that:

$$P\, v_1 = \begin{bmatrix} a_n\, L - 2k_\alpha\, s_n\, I_n & -s_n\, I_n \\ b_n\, L^2 & c_n\, L \end{bmatrix} \begin{bmatrix} \mathbf{1}_n \\ -2k_\alpha \mathbf{1}_n \end{bmatrix} = \mathbf{0}_{2n}.$$

Now, consider the imaginary eigenvalue $\lambda_2 = 2s_n j$. By replacing v_2 into the eigenvalue equation we obtain

$$\begin{bmatrix} a_n\, L - 2k_\alpha\, s_n\, I_n & -s_n\, I_n \\ b_n\, L^2 & c_n\, L \end{bmatrix} \begin{bmatrix} \psi_1 \\ f_{n,2}(k_\alpha)\psi_1 \end{bmatrix} = 2s_n j \begin{bmatrix} \psi_1 \\ f_{n,2}(k_\alpha)\psi_1 \end{bmatrix},$$

Note that L and L^2 (which are both circulant matrices) satisfy, respectively, $L\psi_1 = (e^{2\pi j/n} - 1)\psi_1 = (-2s_n j(c_n + js_n))\psi_1$, and $L^2\psi_1 = (e^{2\pi j/n} - 1)^2\psi_1 = -4s_n^2 e^{2\pi j/n}\psi_1$; hence, v_2 is an eigenvector for P if and only if:

$$
\begin{aligned}
(a_n(e^{2\pi j/n}-1)-2k_\alpha s_n)\psi_1+2b_n e^{j\pi/n}s_n\psi_1 &= 2s_n j\psi_1 && (44)\\
-4b_n s_n^2(c_n+js_n)^2\psi_1-c_n(-2s_n j(c_n+js_n))2b_n e^{j\pi/n}\psi_1 &= -4b_n e^{j\pi/n}s_n j\psi_1 && (45)
\end{aligned}
$$

By using the identities in equation (40), the first condition can be verified according to

$$
\begin{aligned}
2s_n(-c_n+k_\alpha s_n)je^{j\pi/n}-2s_n k_\alpha+2s_n b_n e^{j\pi/n} &= 2s_n j,\\
2((c_n-k_\alpha s_n)j-(k_\alpha+j)(c_n-js_n))e^{\pi j/n} &= -2b_n e^{j\pi/n},\\
-2(s_n+k_\alpha c_n)e^{\pi j/n} &= -2b_n e^{j\pi/n}.
\end{aligned}
$$

Similarly, the condition in equation (45) can be verified according to

$$
\begin{aligned}
-2b_n s_n^2(c_n+js_n)^2+2c_n(js_n(c_n+js_n))b_n e^{j\pi/n} &= -2b_n e^{j\pi/n}s_n j,\\
-s_n(c_n+js_n)+c_n(j(c_n+js_n)) &= j,\\
j(s_n^2+c_n^2) &= j.
\end{aligned}
$$

Similar arguments hold for λ_3 and v_3 (which are complex conjugates of λ_2 and v_2). This concludes the proof. □

C. Proof that $v_i \notin T_{(\varrho^*,\varphi^*)}\tilde{\mathcal{M}}$

Proof: It is enough to prove that at least one of the components of $G \cdot v_i$ is nonzero. The proof that $G \cdot v_1 \neq 0$ is trivial. We proceed to show that $\nabla g_1 \cdot v_2 \neq 0$, i.e.:

$$
\left[1 \ \cos\left(\frac{2\pi}{n}\right) \ \ldots \ \cos\left(\frac{2\pi(n-1)}{n}\right) \ -\sum_{i=2}^{n} r\sin\left(\frac{2\pi(i-1)}{n}\right) \ \ldots \ -r\sin\left(\frac{2\pi(n-1)}{n}\right) \ 0\right]\left[\begin{array}{c}\psi_1\\ -2b_n e^{j\pi/n}\psi_1\end{array}\right]
$$
$$
= (\nabla_\varrho g_1)\cdot\psi_1+(\nabla_\varphi g_1)\cdot(-2b_n e^{j\pi/n}\psi_1)\neq 0.
$$

Both terms in the above sum can be shown to be real and positive. For the first term we have that:

$$
\begin{aligned}
(\nabla_\varrho g_1)\cdot\psi_1 &= \sum_{k=0}^{n-1}\cos(2\pi k/n)(\cos(2\pi k/n)+j\sin(2\pi k/n))\\
&= \sum_{k=0}^{n-1}\cos^2(2k\pi/n)+j\sum_{k=0}^{n-1}2\sin(k\pi/n)=\sum_{k=0}^{n-1}\cos^2(2k\pi/n)\in\mathbb{R}_{>0}.
\end{aligned}
$$

For the second term we have:

$$
\begin{aligned}
(\nabla_\varphi g_1)\cdot(-2b_n e^{j\pi/n}\psi_1) &= \sum_{k=0}^{n-1}\sum_{i=k+1}^{n} \sin(2\pi k/n) 2b_n e^{j\pi/n} e^{2\pi k/n} \\
&= 2b_n \sum_{k=0}^{n-1} a_k e^{(2k+1)\pi j/n},
\end{aligned}
$$

where $a_k = \sum_{i=k+1}^{n} \sin(2\pi i/n) = -\sum_{i=1}^{k}\sin(2\pi i/n)$. Now we show that $\sum_{k=0}^{n} a_k e^{(2k+1)\pi j/n} > 0$. First, consider the following facts:

$$
\begin{aligned}
a_k &\le 0 \quad \forall k, \\
a_{k+1} &= a_k - \sin(2\pi(k+1)/n) < a_k \quad \text{for} \quad 0 \le k < n/2-1, \\
a_{\lfloor (n-1)/2 \rfloor} &< a_k \quad \forall k \neq \lceil (n-1)/2 \rceil, \\
a_{n-k} &= -\sum_{i=1}^{n-k} \sin(2\pi i/n) = \sum_{m=k+1}^{n} \sin(2\pi m/n) = a_k, \\
\sum_{k=0}^{n-1} a_k e^{(2k+1)\pi j/n} &= \sum_{k=0}^{\lfloor (n-1)/2 \rfloor} (a_k e^{k\pi j/n} + a_{n-k} e^{-k\pi j/n}) + q a_{(n-1)/2} \\
&= \sum_{k=0}^{\lfloor (n-1)/2 \rfloor} a_k (e^{\pi k j/n} + e^{-k\pi j/n}) + q a_{(n-1)/2} \\
\sum_{k=0}^{n-1} e^{(2k+1)\pi j/n} &= \sum_{k=0}^{\lfloor (n-1)/2 \rfloor} (e^{\pi k j/n} + e^{\pi - kj/n}) + q = 0
\end{aligned}
$$

where $q = 0$ if n is even. Then,

$$
\sum_{k=0}^{n-1} a_k e^{(2k-1)\pi j/n} > \sum_{k=0}^{n-1} a_{\lfloor (n-1)/2 \rfloor} e^{(2k-1)\pi j/n} = 0.
$$

Since $b_n = (s_n + k_\alpha c_n) > 0$, we have that $\nabla_\varphi g_1 \cdot (-2b_n e^{j\pi/n}) \in \mathbb{R}_{>0}$.

The proof for $G \cdot v_3 \neq 0$ is analogous; in particular, it requires to show that $j\nabla_\varrho g_2 \cdot \psi_1 \in \mathbb{R}_{>0}$ and $j\nabla_\varphi g_2 \cdot (-2b_n e^{j\pi/n}\psi_1) \in \mathbb{R}_{>0}$.

$\square$

References

[1]Carpenter J., "Benchmark Problems for Spacecraft Formation Flying Missions", *AIAA Guidance, Navigation, and Control Conference and Exhibit*, Austin, Texas, Aug. 11-14, 2003.

[2]Fridlund, C.V.M. , " Darwin: The Infrared Space Interferometry Mission", *Advances in Space Research*,

ESTEC, Noordwijk, The Netherlands. Vol. 34, No.3, 2004, pp. 613-617.

[3]Chakravorty, S.,Ramirez, J., Chakravorty, S., "On the Fuel Optimal of Multispacecraft Interferometric Imaging systems", *Journal of Guidance, Control and Dynamics*, Vol.30 No.1, Jan-Feb 2007. pp 227-236.

[4]Pavone, M., Frazzoli, E. "Decentralized policies for geometric pattern formation and path coverage". *Journal of Dynamic Systems, Measurement, and Control*. Vol.129, Issue 5, 2007 pp. 633-643.

[5]Schweigart, S., Sedwick, R. " High-Fidelity Linearized J_2 Model for Satellite Formation Flight". *Journal of Guidance, Control and dynamics*, Vol. 25, No. 6, 2002. pp. 1073-1080.

[6]Justh E. W. and Krishnaprasad, P. S., " Steering laws and continuum models for planar formations", *Proc. 42nd IEEE Conf. Decision and Control*, Maui, HI, Dec. 2003, pp. 3609-3614.

[7]Jadbabaie, A., Lin J. and Morse, A. S., " Coordination of groups of mobile autonomous agents using nearest neighbor rules", *IEEE Trans. Automat. Contr.*, Vol. 48, June 2003, pp. 988-1001.

[8]Vicsek, T., Czirok, A., Ben-Jacob, E., Cohen, I. and Schochet, O., " Novel type of phase transitions in a system of self-driven particles", *Physical Review Letters*, Vol. 75, 1995, pp.1226-1229.

[9]Olfati-Saber, R.,and Murray, R. M. , " Flocking with Obstacle Avoidance: Cooperation with Limited Communication in Mobile Networks", *Proc. of the 42nd IEEE Conference on Decision and Control*, 2003.

[10]Leonard, N., and Friorelli, E. , " Virtual leaders, artificial potentials and coordinated control of groups", *Proc. 39th IEEE Conference on Decision and Control*, Orlando, FL, 2001.

[11]Lin, Z., Broucke, M. , and Francis, B., " Local control strategies for groups of mobile autonomous agents", *IEEE Trans. on Automatic Control*, Vol.49, Issue 4, 2004, pp.622-629.

[12]Marshall, J. A., Broucke M. E. , and Francis, B. A., " Formations of Vehicles in Cyclic Pursuit", *IEEE Transactions On Automatic Control*, Vol.49, No.11, November 2004.

[13]Marshall, J. A., Broucke M. E., and Francis, B. A. , " Pursuit Formations of Unicycles", *Automatica*, Vol.41, No.12, December 2005.

[14]Paley, D. A. , Leonard, N., Sepulchre, R., " Stabilization of symmetric formations to motion around convex loops". *Systems & Control letters*, Vol.57, 2008. pp. 209-215.

[15]Ren W. " Collective motion from consensus with Cartesian coordinate coupling - Part I: Single-integrator kinematics". *Proc. 47th IEEE Conference on Decision and Control*, Cancun, Mexico, Dec. 2008, pp. 1006 - 1011.

[16]Ren W. " Collective motion from consensus with Cartesian coordinate coupling - Part II: Double-integrator dynamics". *Proc. 47th IEEE Conference on Decision and Control*, Cancun, Mexico, Dec. 2008, pp. 1012 - 1017.

[17]Scharf, D.P., Hadaegh, F.Y., Ploen, S.R., " A survey of spacecraft formation flying guidance and control. Part II: control", *Proceeding of the American Control Conference*, Vol. 4, 2004, pp. 2976-2985.

[18]Chung, S.-J., Ahsun, U. and Slotine, J.-J.E., "Application of synchronization to formation flying spacecraft: Lagrangian approach," *Journal of Guidance, Control, and Dynamics*, Vol. 32, pp. 512-526, March 2009.

[19]Davis, P. J. , " Circulant Matrices", 2nd ed. New York: Chelsea, 1994.

[20]Gray, R. M.," Toeplitz and Circulant Matrices: A review", *Foundations and Trends in Communications and Information Theory*, Vol.2, Issue 3, 2006, pp. 155-239.

[21]*http://ssl.mit.edu/spheres/*

List of Figures